The T-box Transcription Factor Eomesodermin Governs Hemogenic Competence of Yolk-Sac Mesodermal Progenitors

Luke T.G. Harland[1], Claire S. Simon[1,7], Anna D. Senft[1,8], Ita Costello[1], Lucas Greder[2], Ivan Imaz-Rosshandler[3,4], Berthold Gottgens[3], John C. Marioni[4,5,6], Elizabeth K. Bikoff[1], Catherine Porcher[2], Marella de Bruijn[2,9], Elizabeth J. Robertson[1,9]

[1]Sir William Dunn School of Pathology, University of Oxford, South Parks Road, Oxford, OX1 3RE, UK

[2]MRCMolecular Haematology Unit, MRC Weatherall Institute of Molecular Medicine, University of Oxford, John Radcliffe Hospital, Oxford, OX3 9DS, UK

[3]Wellcome-MRC Cambridge Stem Cell Institute, Jeffrey Cheah Biomedical Centre, University of Cambridge, Cambridge, CB2 0AW, UK

[4]European Molecular Biology Laboratory, European Bioinformatics Institute (EMBL-EBI), Wellcome Genome Campus, Cambridge, CB10 1SD, UK

[5]Wellcome Sanger Institute, Wellcome Genome Campus, Cambridge, CB10 1SA, UK

[6]CRUK Cambridge Institute, University of Cambridge, Robinson Way, Cambridge, CB2 0RE, UK

Abstract

Extra-embryonic mesoderm (ExM), the earliest cells that traverse the primitive streak (PS), give rise to the endothelium as well as hematopoietic progenitors in the developing yolk-sac (YS). How a specific subset of ExM becomes committed to a hematopoietic fate remains unclear. Here we demonstrate using an embryonic stem cell (ESC) model that transient expression of the T-box transcription factor Eomesodermin (Eomes) governs hemogenic competency of ExM. Eomes regulates the accessibility of enhancers that SCL normally utilizes to specify primitive erythrocytes and is essential for the normal development of Runx1^{+} hemogenic endothelium. Single-cell-RNA-seq suggests that Eomes loss-of-function profoundly blocks formation of blood progenitors but not specification of Flk-1^{+} hematoendothelial progenitors. Our findings place Eomes at the top of the transcriptional hierarchy regulating early blood formation and suggest that

[9]Corresponding authors. (E.J.R Elizabeth.robertson@path.ox.ac.uk; M.dB marella.debruijn@imm.ox.ac.uk).
[7]Current address: Developmental Biology Program, Memorial Sloan Kettering Cancer Centre, New York, NY10065, USA
[8]Current address: National Institutes of Health/NICHD, 6 Center Drive, Bethesda, MD 20892, USA

hemogenic competence is endowed earlier during embryonic development than previously appreciated.

Introduction

The process of gastrulation generates the three primary embryonic germ layers, namely mesoderm, ectoderm and definitive endoderm. Beginning at embryonic day 6 (E6.0), in response to local signaling cues, pluripotent epiblast cells on the prospective posterior side of the embryo undergo a process of epithelial-to-mesenchymal transition allowing them to delaminate and migrate within the PS[1]. The first cells that traverse the PS include progenitors of the ExM that migrate proximally to generate the developing YS[1–3]. ExM subsequently differentiates into endothelial cells that form the YS vasculature as well blood progenitors that sustain growth and development of the post-implantation embryo[3, 4].

Hematopoietic progenitors initially form at E7.5 to generate nucleated primitive erythrocytes within the distally located YS blood islands (BI)[3]. A day later a second wave of blood progenitors arise from a subset of endothelial cells present within the developing YS vasculature[5]. This so-called hemogenic endothelium (HE) undergoes an endothelial-to-hematopoietic transition (EHT) whereby cells round up, detach from the endothelial layer and enter the blood stream[6–8]. Hematopoietic progenitors derived from YS HE at E8.25 have restricted erythro-myeloid potential and generate enucleated erythrocytes[9] and are therefore designated 'definitive'. Subsequently, at E10.5 a third wave of hematopoietic progenitors including definitive hematopoietic stem cells (HSC) arise from HE in vascular beds of the dorsal aorta and vitelline/umbilical arteries[7, 10].

Understanding the transcriptional hierarchy that guides hematopoiesis during embryogenesis is essential for the generation of hematopoietic progenitors from pluripotent stem cell sources *in vitro* [11, 12]. Of particular interest is how HE is specified as this represents a critical early step in the generation of definitive hematopoietic cells including the HSC. Only a few transcriptional regulators that impact hematopoietic output from HE have been identified, including the transcription factors (TF) SCL and Runx1 that play key roles during embryonic hematopoiesis. SCL is required for the specification of the blood fate and the generation of HE and all hematopoietic cells[13–17]. In contrast, Runx1 is non-essential for the generation of HE or primitive erythrocytes/megakaryocytes but is essential for EHT and the production of all definitive hematopoietic stem and progenitor cells[18].

Here we report that the T-box TF Eomes is transiently expressed in ExM progenitors that generate virtually all YS hematopoietic and endothelial cells. Using an ESC differentiation system, we find that Eomes is essential for the production of primitive erythrocytes and Runx1$^+$ HE. Eomes is expressed prior to both SCL and Runx1 during mesoderm patterning. Single-cell RNA-seq (scRNAseq) comparisons to *in vivo* hematoendothelial development strongly suggest the block in hematopoietic development in Eomes loss-of-function cultures occurs after the specification of Flk-1$^+$/SCL$^+$ hematoendothelial progenitors. ATAC-Seq experiments reveal that Eomes governs the accessibility of Runx1 enhancers as well as *cis*-regulatory regions that SCL normally utilizes to specify primitive erythrocytes. ChIP-seq experiments demonstrate that Eomes occupies Runx1 *cis*-regulatory regions and coordinates

the development of hemogenic competent mesoderm in the context of Activin/Nodal and Tead-Yap signaling. Finally, re-expression of Runx1 in Eomes-null endothelial cultures is sufficient to rescue the block in EHT and definitive blood production. Collectively, these experiments demonstrate that Eomes sits at the top of the transcriptional hierarchy, functioning upstream of Runx1 expression and SCL functional activity, to promote hemogenic competence of the YS mesodermal lineage.

Results

Eomes expression transiently marks the proximal epiblast, PS and Flk-1^{+} ExM progenitors that give rise to hematopoietic and endothelial lineages of the YS

The first wave of cells to traverse the PS give rise to ExM that migrates proximally, displacing the overlying extra-embryonic ectoderm (ExE) to form the inner layer of the developing YS[2, 3]. Subsequently these cells generate the BI containing primitive erythrocytes and endothelial cells that give rise to the YS vascular network[3] (Fig. 1a). The T-box TF factor brachyury (T) is expressed in the PS and nascent mesoderm, including the hemangioblast, a multipotent progenitor that generates hematopoietic and endothelial cells[19]. Flk-1 also marks the hemangioblast[19] and *in vivo* fate mapping studies demonstrate that YS hematopoietic and endothelial cells are derived from Flk-1^{+} ExM[20].

Here we observed that Eomes expression is detectable in proximal epiblast/PS cells at early/mid PS stages (E6.5) prior to widespread T expression (Fig. 1b,c). Additionally, at mid-streak (E6.5) stages a population of Flk-1^{+} migratory mesoderm co-expressed Eomes in the extraembryonic region (Extended Data Fig. 1a). To test whether Eomes expressing progenitors contribute to the ExM at later stages we performed short-term lineage tracing experiments using an Eomes[GFP/+] reporter line[21]. At E7.5 Eomes-GFP^{+} cells detected within the YS BIs co-expressed Flk-1 (Fig. 1d) and the ExM/hematopoietic marker Runx1 (Fig. 1e). However, this reflects GFP perdurance as endogenous Eomes protein was no longer detectable in Eomes-GFP[+] (Fig. 1f) or Flk-1^{+} cells in the YS at this stage (Extended Data Fig. 1b).

To examine contributions made by Eomes-expressing cells to YS vascular and hematopoietic lineages we generated an *Eomes[iCre]* reporter allele (Extended Data Fig. 2a-e) and performed long-term lineage tracing experiments. *Eomes[iCre/+]* males were mated to females carrying the *ROSA26[R]* allele[22] and the resulting embryos stained for LacZ expression. At E8.5 and E9.5 virtually all the YS hematopoietic and endothelial cells in *Eomes[iCre]; ROSA26[R]* embryos were LacZ[+] (Fig. 1g). Thus, we conclude that transient Eomes expression marks ExM progenitors that give rise to the YS hematopoietic and endothelial compartments.

To assess Eomes functional contributions we analyzed E7.5 embryos carrying an epiblast-specific *Eomes* deletion (*Eomes* [CA/N];Sox2.Cre)[23] that disrupts delamination of nascent mesoderm[23]. In contrast to wild-type embryos, *Eomes* [Epi] mutant embryos fail to induce expression of Flk-1 and ER71, genes essential for YS hematopoiesis and vasculogenesis[24–26] (Extended Data Fig. 2f). Thus, Eomes expression in the epiblast is essential for the generation of ExM.

Eomes is expressed transiently in hematovascular progenitors prior to the onset of SCL and Runx1 expression during hematopoietic differentiation

To circumvent *in vivo* morphogenetic defects caused by Eomes functional loss, we exploited an *in vitro* ESC differentiation protocol[27, 28] to promote the formation of YS-like hematopoietic and endothelial progenitors via the staged addition of growth factors to embryoid bodies (EB) under serum free conditions (Fig. 2a-c). Eomes[21], SCL[29] and Runx1 (Extended Data Fig. 3a,b) expression were analyzed utilizing ESC reporter lines. Dissociated EBs were stained for Flk-1 and PdgfRa, markers that distinguish hematovascular mesoderm (Flk-1^{hi}/PdgfRa$^-$), primitive/cardiac mesoderm (Flk-1$^+$/PdgfRa$^+$), and paraxial mesoderm (Flk-1$^-$/PdgfRa$^+$) and the hematopoietic marker CD41[26, 30–34] (Fig. 2d,e). Eomes-GFP was detectable at day 3 prior to expression of Flk-1/PdgfRa. The majority of cells at day 4, including the Flk-1^{hi}/PdgfRa$^-$ hematovascular mesoderm compartment, express Eomes-GFP (Fig. 2d). 24 hours later Eomes-GFP$^+$ cells comprise roughly half the Flk-1^{hi}/PdgfRa$^-$ compartment (Fig. 2d). In contrast, developing CD41$^+$ hematopoietic cells are predominantly Eomes-GFP$^{lo/-}$ (Fig. 2e).

At day 4 SCL-mCherry is exclusively expressed within the Flk-1^{hi}/PdgfRa$^-$ compartment (Fig. 2d). At day 5 hematopoietic cells co-express CD41 and SCL-mCherry and downregulate Flk-1 expression (Fig. 2d,e). Runx1-Venus is also expressed in CD41$^+$ hematopoietic cells (Fig. 2e). However, in contrast to SCL-mCherry, Runx1-Venus expression is restricted to cells that weakly express Flk-1 within the Flk-1^{hi}/PdgfRa$^-$ compartment at day 4/5 (Fig. 2d).

Consistent with above results, differentiation trajectories constructed using scRNAseq data from E6.5 to E8.5 mouse embryos[15] reveal dynamic Eomes expression in mesoderm/ hematoendothelial progenitors that give rise to SCL and Runx1 expressing hematopoietic and endothelial cells (Fig. 2f). Thus, we conclude Eomes is transiently expressed, prior to SCL and Runx1, in hematovascular mesoderm progenitors.

Eomes functional loss disrupts primitive and definitive hematopoiesis but not endothelial development

Next, we examined the ability of Eomes-null ESC[23] to generate hematovascular mesoderm (Fig. 3a). Eomes-null EBs contain a detectable but decreased number of Flk-1^{hi}/PdgfRa$^-$ cells at day 4/5 and lack Flk-1$^+$/PdgfRa$^+$ progenitors at day 4, reflecting Eomes requirements for cardiac mesoderm specification[35, 36] (Fig. 3b). RNA-Seq experiments performed at day 4 reveal that Eomes-null Flk-1^{hi}/PdgfRa$^-$ cells express SCL, ER71, Gata2, Lmo2, Tek, Cdh5, Fli1 and CD31 (Fig. 3c), suggesting that Eomes is non-essential for specification of hematovascular mesoderm. In contrast, EHT regulators including Runx1 and Gfi1b, and genes expressed in erythroid cells (Gata1 and Hbb-bh1) were downregulated (Fig. 3c).

To further examine Eomes functional requirements we cultured EBs for three more days in pro-hematopoietic conditions (Fig. 3a, red). Wild-type cultures robustly form hematopoietic progenitors co-expressing c-Kit, and/or CD41 and CD45, and generate primitive/definitive erythrocyte and myeloid/mixed hematopoietic colonies (Fig. 3d,e). In contrast, Eomes-null

cultures lack the ability to form CD41$^+$/CD45$^+$ cells and hematopoietic colonies (Fig. 3d,e). These cultures contain CD31$^+$/Cdh5$^+$ endothelial cells (Fig. 3f) and express normal levels of endothelial marker genes Cdh5, Flk-1, Flt-1 and Fli-1 (Fig. 3,g). However, SCL, Runx1, PU.1, Gata1 and Hbb-bh1 transcripts at day 6 were markedly downregulated confirming a block in hematopoiesis (Fig. 3g).

To further explore Eomes functional contributions Flk-1^{hi} cells were isolated at day 5 and plated on Matrigel under conditions known to promote HE development[37] (Fig. 3a, blue). By day 8 wild-type Flk-1^{hi} cells give rise to patches of adherent Cdh5$^+$/c-Kit$^+$ HE cells that actively undergo EHT to generate semi-adherent and floating CD41$^+$/CD45$^+$ hematopoietic cells (Fig. 3h,i). Eomes-null Flk-1^{hi} cells generate Cdh5$^+$/c-Kit$^+$ endothelium but these cells fail to efficiently undergo EHT and lack expression of the hematopoietic markers CD41/ CD45 (Fig. 3i). Thus, we conclude Eomes is dispensable for the generation of endothelial cells but is essential for both primitive and definitive hematopoietic development.

Eomes is essential for the generation of Runx1$^+$ hemogenic endothelium

Defects observed above in Eomes-null ESCs closely resemble those reported for SCL mutants[13]. Therefore, next we re-generated the Eomes-null allele in ESCs that contain an SCL reporter allele[29] (Extended Data Fig. 4a-c) to directly test Eomes requirements for SCL expression. At day 5 of differentiation many Eomes-null Flk-1^{hi}/PdgfRa$^-$ cells are SCL-mCherry$^+$ (Fig. 4a) and a day later a high proportion of c-Kit$^+$/Cdh5$^+$ cells expressed wild-type levels of SCL-mCherry (Fig. 4b). Thus, the block in primitive and definitive hematopoiesis observed in Eomes-null cultures cannot be explained simply due to loss of SCL expression.

Runx1 expression is required for EHT and the generation of definitive hematopoietic cells[18]. To assess whether the block in definitive hematopoiesis in Eomes-null cultures reflects the absence of HE, we disrupted Eomes expression in the Runx1-Venus reporter ESCs (Extended Data Fig. 4a-c). At day 5 Eomes-null EBs almost entirely lack Runx1-Venus expression (Fig. 4c). At day 8, Runx1-Venus expression normally marks a CD41$^{-/lo}$ HE subset within the c-Kit$^+$/Cdh5$^+$ compartment (Fig. 4d, blue gate). Upon EHT, cells upregulate CD41, generating Runx1-Venus$^+$/CD41$^+$ hematopoietic cells (Fig. 4d, green gate). Strikingly, Eomes-null EHT cultures lack Runx1-Venus$^+$cKit$^+$/Cdh5$^+$ HE (Fig4d, blue gate). Eomes-null Runx1-Venus day 5 EBs and day 8 EHT cultures lack clonogenic progenitors for primitive erythrocyte and definitive erythro-myeloid lineages, respectively (Fig. 4e), as well as Cdh5$^-$/CD41$^+$/Runx1-Venus$^+$ cells (Fig. 4d, orange gate) and budding cells (Fig. 4f). We conclude that the block in definitive hematopoiesis in Eomes-null EHT cultures is associated with the loss of Runx1+ HE.

To test whether Eomes regulates Runx1 expression in a cell autonomous fashion, we performed co-culture experiments. Wild-type ESCs were mixed with Runx1-Venus or Eomes-null Runx1-Venus ESCs (Extended Data Fig. 3c). Wild-type:Runx1-Venus co-cultures at day 6 contain CD41$^+$ hematopoietic cells that are Runx1-Venus$^+$. In contrast, Runx1-Venus expression in CD41$^+$ cells is barely detectable in Eomes-null Runx1-Venus:wild-type co-cultures. These results strongly suggest that Eomes promotes robust induction of Runx1 expression in a cell-autonomous fashion during hematopoiesis.

Eomes influences chromatin accessibility at SCL bound enhancers in hematovascular mesoderm

To investigate Eomes-dependent chromatin accessibility we performed ATAC-Seq[38] analysis of day 4 wild-type and Eomes-null Flk-1^{hi}/PdgfRa[-] hematovascular mesoderm. We identified changes at 4180 genomic locations corresponding to ~7% of all accessible sites (Fig. 5a). The majority of sites (>85%) showing reduced chromatin accessibility in Eomes-null cells were located in distal intergenic regions (Fig. 5a) and are enriched for binding motifs for hematopoietic regulators such as Gata1/2, SCL, Erg, Ets1, Fli1, Runx1, Meis1 and Gfi1b (Fig. 5b). Strikingly, when these peaks were compared to published ChIP-Seq datasets from Flk-1^{+} cells generated using a hematopoietic differentiation protocol[39], we found that the majority of Eomes-dependent sites with reduced accessibility were enriched for enhancer marks (H3K4Me1 and H3K27Ac) and SCL occupancy (Fig. 5c). Moreover, sites showing reduced accessibility that correlate with SCL occupancy are enriched for genes related to hematopoietic development (Fig. 5d). Of these 231 are associated with downregulated genes in Eomes-null Flk-1^{hi}/PdgfRa^{-} cells including Gata1 and Nfe2, which are critical for primitive erythrocyte development and those governing EHT and definitive hematopoiesis, namely Runx1, Gfi1/1b, Ikzf1 and Myb (Fig. 5e). Many of the changes in chromatin accessibility map to previously identified enhancer regions at these loci (Fig. 5f)[40, 41]. Consistent with results above there was no noticeable impact on chromatin accessibility at the SCL locus (Fig. 5f). These results demonstrate that Eomes regulates accessibility at SCL-bound *cis*-regulatory elements.

Sites co-occupied by Eomes, Tead4 and Smad2/3 are transiently marked by H3K27Ac during early stages of hematopoietic development

To facilitate identification of Eomes target genes we generated ESCs expressing C-terminally V5-tagged Eomes (Eo-V5) (Extended Data Fig. 5a-c,f). Intracellular flow cytometry demonstrated that Eo-V5 expression peaked at day 4 during hematovascular mesoderm development (Extended Data Fig. 5d). Eo-V5 is expressed broadly in primitive/cardiac mesoderm (Flk-1^{+}/PdgfRa[+]) as well as a subset of developing hematovascular (Flk-1^{hi}/PdgfRa^{-}) mesodermal cells (Extended Data Fig. 5e). Homozygous Eo-V5 EB cultures generate Flk-1^{+}/PdgfRa^{+} primitive/cardiac mesoderm and c-Kit^{+}/CD41^{+} hematopoietic progenitors, confirming that Eomes-V5 functions normally (Extended Data Fig. 5g).

We used two independent Eo-V5 ESC clones (CL A and CL B) for ChIP-Seq analysis. V5-Eomes bound genomic regions common to both clones (Fig. 6a) were highly enriched for the Eomes binding motif[42] and were predominantly located >5 kb from transcriptional start sites (Fig. 6b). 30% of genes linked to ChIP peaks were found to be mis-regulated in day 4 Flk-1^{hi}/PdgfRa[-] Eomes-null cells including transcriptional regulators (Runx1, Mixl1, Klf5, Pbx1, Tbx3, Foxf1, Meis2) and signaling molecules (Dkk1, Gli2, Fzd7, Lefty2) controlling hematovascular development[27, 43-48] (Fig. 6c).

Next, we examined published ChIP-Seq datasets[49, 50] to assess co-occupancy by transcriptional regulators, DNase hypersensitivity sites and local histone marks during hematopoietic differentiation (Fig. 6d). The majority of Eomes occupied sites were marked

by H3K27Ac and display DNase hypersensitivity in hemangioblasts (T^+/Flk-1^+) but not hematopoietic progenitors ($CD41^+$) (Fig. 6d). Strikingly, many are also co-bound by Smad2/3 and the TF Tead4 (Fig. 6d). Overlapping Eomes, Smad2/3 and Tead4 peaks identified 72 sites corresponding to genes associated with hematopoiesis and mesoderm development (Fig. 6e). We observe co-occupancy at genes down-regulated in day 4 Flk-1^{hi}/PdgfRa$^-$ Eomes-null EBs (Fig 6c) including the promoter region of Mixl1, previously shown to regulate the generation of Flk-1+ hematopoietic mesoderm[32, 42, 44, 51] and putative *cis*-regulatory elements controlling Dkk1 and Tbx3 expression (Fig. 6h). Eomes, Tead4 and Smad2/3 co-occupy a potential cis-regulatory region 181kb upstream of the Runx1 TSS locus marked transiently by H3K27Ac (Fig. 6h). Recent ChIP-seq experiments[51] confirm Eomes occupancy at this -181kb region (Extended Data Fig. 6) as well as the Runx1 proximal promoter (P2) that is active in HE[52] and several Runx1 enhancers (+110, +171, +204, -327) known to regulate expression during hematopoiesis[40, 53] (Extended Data Fig. 6). Eomes induction also rescues Runx1 expression in this context[51] suggesting that Eomes directly regulates Runx1 expression.

Finally, we overlaid our day 4 Eomes ChIP-Seq peaks with the ATAC-Seq peaks with reduced accessibility in day 4 Flk-1^{hi}/PdgfRa$^-$ Eomes-null mesoderm as well SCL ChIP-Seq peaks from day 4 wild-type Flk-1^+ EBs[39]. Very few of the ATAC peaks (33/3629) or SCL ChIP Peaks (19/4393) are bound by Eomes at day 4 (Extended Data Fig. 7a). Interestingly, Eomes ChIP peaks are accessible at early mesodermal (T^+/Flk-1^-) stages of development and become marked by H3K27Ac after the onset of Flk-1 expression[49] (Extended Data Fig. 7b). By contrast, Eomes-dependent ATAC peaks normally bound by SCL only become accessible in the hemangioblast (T^+/Flk-1^+) population[49] (Extended Data Fig. 7b). These results suggest that Eomes-dependent SCL bound *cis*-regulatory regions become accessible only subsequent to Eomes functional activity at earlier stages in the hematopoietic differentiation pathway.

Single-cell RNA-Seq reveals the stage at which hematopoietic development is blocked in Eomes loss-of-function cultures

To characterize the stage when hematopoietic development is blocked in Eomes loss-of-function cultures we performed scRNA-seq on Eomes-null and wildtype Flk-1^{hi}/PdgfRa$^-$ populations at day 4 and day 5 (Extended Data Fig. 8a). An integrated analysis[54] was performed that allowed uniform manifold approximation and projection (UMAP), and the identification of 13 clusters (Extended Data Fig. 8). Cluster identities were determined by comparing marker genes conserved across genotypes (Supplementary Table 1) to those previously used to document discrete cell populations present in E6.5 to E8.5 mouse gastrulation atlas[15]. Additionally, we were able to map the *in vitro* derived cells onto the mouse gastrulation atlas[15], allowing us to transfer cell identities and embryonic stages onto our scRNA-seq dataset (Fig. 7a-d).

Cells from day 4 EBs were found mainly in clusters 2-6 (Extended Data Fig. 8b,c) and resembled *in vivo* mixed mesoderm and hematoendothelial progenitors (Fig. 7a) that express T, Mixl1, ER71 and SCL (Fig. 7b, Extended Data Fig. 8e). By contrast, day 5 cells mainly contributed to clusters 7-13 (Extended Data Fig. 8b,c) that resembled *in vivo*

hematoendothelial progenitors, endothelium, allantois and blood progenitors 1 and 2 (Fig. 7a) and expressed varying levels of Runx1, Gata1, Cdh5, Pecam1 and Spin2c (Fig. 7b, Extended Data Fig. 8e). Day 4 Eomes-null and wild-type cells contributed relatively equally to mesodermal/hematoendothelial progenitor clusters 2-6 (Extended Data Fig. 8c). By contrast, day 5 Eomes-null cells predominately contributed to the hematoendothelial progenitor, endothelial and allantoic clusters (9-13) at the expense of blood progenitor clusters (7 and 8; Extended Data Fig. 8c). The exceptional Eomes-null cells contributing to clusters 7 and 8 expressed hematovascular genes SCL, ER71, Cdh5 and CD31 but had reduced expression of EHT regulators Runx1/Gfi1b (Extended Data Fig. 8e,f). Interestingly, many Eomes-null Flk-1^{hi}/PdgfRa$^-$ cells display transcriptional profiles similar to endothelial cells and hematoendothelial progenitors from E7.75-E8.5 mouse embryos (Fig. 7d). Mapping cells onto the *in vivo* hematoendothelial differentiation trajectory of the mouse gastrulation atlas[15] (cf. Fig. 2f) suggests that the developmental block in Eomes-null cultures reflects the failure of hematoendothelial progenitors to transition into blood progenitors 1/2 (Fig. 7e).

Runx1 re-expression in Eomes-/- EHT cultures rescues the production of definitive hematopoietic progenitors

Day 5 Eomes-null Flk-1^{hi}/PdgfRa$^-$ cultures contain endothelial cells (Fig. 7a,e, Extended Data Fig. 8c) but could not form Runx1$^+$ HE (Fig. 4d). Both Runx1-null and Eomes-null ESCs generate a Cdh5$^+$/cKit$^+$/CD41^{lo} population (Extended Data Fig. 9a,b). However, this population was absent from equivalent SCL-null cultures (Extended Data Fig. 9a,b). To further characterize Eomes functional contributions in relation to Runx1 we deleted Eomes in the context of a Runx1 inducible ESC line[14, 52] (iRunx1; Runx1-null with a doxycycline (dox) inducible Runx1b cDNA inserted into the ROSA26 locus) (Extended Data Fig. 4d,e). This strategy enabled us to drive Runx1 expression in Eomes-null EHT cultures and perform rescue experiments.

As expected, day 5 iRunx1 Eomes-null EBs generate a Flk-1^{hi}/PdgfRa$^{lo/-}$ population (Fig. 8,a) but lack primitive erythrocyte progenitors (Fig. 8b), highlighting differences in requirements for Runx1 and Eomes during primitive erythropoiesis. As expected[52], rescuing EHT and generation of functional hematopoietic progenitors via enforced Runx1 expression is highly dose-dependent (Fig. 8c,d). Titration experiments establish that the addition of 90 ng/mL of dox from day 6-8 in iRunx1 Eomes +/+ EHT cultures efficiently rescues generation of definitive erythro-myeloid clonogenic progenitors and Cdh5$^+$/CD41$^+$ and Cdh5$^+$/CD45$^+$ cells (Fig. 8c,d and Extended Data Fig. 9c). Strikingly, these conditions also rescue, albeit less efficiently, the generation of Cdh5$^+$/CD41$^+$ and Cdh5$^+$/CD45$^+$ cells and restore hematopoietic colony formation in iRunx1 Eomes-null cultures (Fig. 8c,d and Extended Data Fig. 8c,d). These findings demonstrate that Eomes acts upstream of Runx1 expression during definitive hematopoiesis.

Discussion

Here we show in the absence of Eomes function Flk-1$^+$ hematoendothelial progenitors are correctly specified. However, upon further differentiation these progenitors cannot transition

into primitive erythrocytes or HE capable of expressing Runx1 and undergoing EHT (Fig. 8e). As judged by scRNA-seq analyses these *in vitro* cells closely resemble those formed *in vivo* when hematopoiesis predominates in the murine YS (E7.5-E8.5). These results highlight the validity of using ESC differentiation cultures as a model of YS hematopoiesis and have allowed us to uncover an essential role for Eomes in this process.

Our ATAC-Seq analysis of Eomes-mutant hematoendothelial progenitors suggests that the block in primitive erythrocyte development occurs because SCL can no longer access the enhancer network through which it normally specifies this lineage. SCL itself is not responsible for governing accessibility of key enhancers that guide this process[39]. These enhancers only become accessible during normal hematopoietic differentiation after the onset of Flk-1 expression. Eomes expression precedes Flk-1/SCL expression during hematoendothelial development. Thus, Eomes potentially functions as a pioneer factor opening SCL enhancers to direct primitive erythrocyte development. Our ChIP-Seq results, however, argue against this idea since the majority of SCL-bound enhancers are not occupied by Eomes.

Recent experiments demonstrate that hemogenic competency of YS endothelial progenitors is actively restrained via BMI1-dependent silencing of Runx1 expression[55]. Additionally, re-expression of Runx1 in non-HE cells is sufficient for their conversion into HE[56, 57]. Therefore, Runx1 is sufficient to promote conversion of YS endothelium towards a hemogenic fate. Here we demonstrate that Eomes acts upstream of Runx1 expression in the HE lineage. Moreover, Runx1 re-expression in Eomes-null cultures rescues the formation of definitive hematopoietic progenitors. ChIP-seq in day 4/5 EBs reveals Eomes occupancy at the Runx1 proximal promoter P2 as well as previously described[40, 53] (+110, +171, +204, -327) and potentially unappreciated (-171/-181) Runx1 enhancers. Furthermore, ATAC-seq demonstrates that hematoendothelial progenitors formed in the absence of Eomes lack chromatin accessibility at enhancers known to drive Runx1 expression in the HE lineage/ sites of definitive hematopoiesis[40, 58] (+3, +23, +110, -322, -327). Considering that YS endothelial cells are derived from Eomes expressing precursors, Eomes likely endows hemogenic competence via its ability to allow Runx1 induction at later developmental stages within the endothelial lineage. Thus, Eomes directs the emergence of an epigenetic landscape that primes HE specification.

The majority of Eomes ChIP-Seq peaks are located at *cis*-regulatory regions active transiently during mesodermal stages of development. Strikingly, many of these Eomes bound sites are co-occupied in similar stage EBs by Tead4 and Smad2/3, TFs that act downstream of Hippo/YAP and Activin/Nodal signalling respectively and have been shown previously to regulate hematopoietic development[27, 28, 31, 49, 59]. Computational analysis shows that sites co-bound by this triad of TFs are associated with genes regulating both mesoderm and blood cell development. Interestingly, disruption of Tead-YAP complex formation profoundly disrupts EHT and the generation of CD41+ cells[49]. Additionally, Tead signalling is essential during mesodermal stages of development, coincident with the onset of Eomes functional activity[49]. It therefore seems likely that Eomes guides hematopoietic mesoderm development in the context of active Activin/Nodal and Tead/YAP signalling.

Fate mapping studies previously suggested that YS hematopoietic and endothelial lineages become segregated within the proximal epiblast, prior to ingression through the PS[2, 60]. The first cells to ingress through the streak predominantly generate primitive hematopoietic cells whilst the second wave generates endothelial precursors[2] that subsequently acquire HE or non-HE fates. Conditional inactivation of Eomes in the PS using a T.Cre deleter strain has no noticeable impact on embryonic development[23]. Therefore, Eomes is likely only required for YS hematopoiesis within a narrow developmental time window at the very outset of gastrulation in the proximal epiblast/PS. The present study makes Eomes the earliest known transcriptional regulator of specifically hematopoietic but not endothelial development, placing it at the top of a transcriptional hierarchy that governs hemogenic competence in the developing mouse gastrula.

Methods

Mouse strains

Animal procedures were performed at the Sir William Dunn School of Pathology, University of Oxford in accordance with Home Office (UK) regulations under the Programme Project License PF2B5F154 and approved by the Oxford Local Animal Welfare and Ethical Committee. Sexually mature males and females (6 weeks +) of the indicated genotypes were intercrossed and pregnant females at the indicated gestational stage were sacrificed for embryo recovery. Eomes[GFP], Rosa26R, Eomes[CA/N];Sox2[Cre] and Flk-1[LacZ] strains were genotyped as previously described[21–24]. The Eomes[iCre] allele was generated using the same strategy as previously described[35]. The iCre coding sequence followed by a polyA cassette and a loxP-flanked neomycin-resistance cassette was introduced into exon 1 between the SphI (translational start) and EagI sites, resulting in removal of ~500bp of the endogenous 5′ coding region of Exon 1. Drug-resistant ESC colonies screened by Southern blot using a 5' external probe[21] were transfected with pMC1.Cre, to remove the selection cassette. Two independent excised ESC clones were used to generate germline chimeras. Offspring were genotyped by PCR using iCre specific primers (Supplementary Table 2).

Immunostaining

E6.5 embryos were fixed in 4% PFA at room temperature (RT) for 30 min. E7.5 embryos and day 4 EBs were fixed in 1% PFA overnight at 4°C. Samples were washed with 0.1% Triton-X, permeabilized with 0.5% Triton-X in PBS for 15 min, washed with 0.1% Triton-X, blocked in 5% donkey serum, 0.2% BSA and 0.1% Triton-X in PBS, incubated with primary antibodies in block solution, washed with 0.1% Triton-X, incubated with fluorophore-conjugated secondary antibodies for 2 hrs at RT, washed with 0.1% Triton-X and counterstained with DAPI. Images were captured with an Olympus FV1000 and collected using Olympus FluoView (version 4.2). Antibodies used are listed in Supplementary Table 3.

Whole-mount in situ hybridization and LacZ staining

E6.5-E7.5 embryos were subject to whole-mount *in situ* hybridization (WISH) using standard protocols[61] with probes against ER71[62], Eomes[23] and iCre (Supplementary Table

4). LacZ staining was performed according to standard protocols[61]. For histology, paraffin-embedded embryos were sectioned (8.0 μm) and counterstained with Nuclear FastRed.

ESC maintenance and differentiation

WT (CCE), Runx1-Venus (E14), SCL-mCherry (J1)[29], Eomes-null (CCE, Runx1-Venus, SCL-mCherry, iRunx1), SCL-null (J1)[17], Runx1-null (J1)[63] and iRunx1[14] ESC lines were maintained in feeder free culture conditions as previously described[35]. 48-72 hrs prior to induction of hematopoietic differentiation cells were cultured in serum free ES media containing 50% Neurobasal Media (Gibco, Cat # 21103049), 50% DMEM/F12 (Gibco, Cat # 11320033), supplemented with 0.5X of both N2 (Gibco, Cat#17502048) and B27 (Gibco, Cat# 17504044), 1%Pen/Strep, 1% glutamine, 0.05% BSA (Gibco, Cat# 15260037), 1 μM PD0325091, 3 μM CHIR99021 and 1000 U/ml LIF. At D0 cells were seeded at a density of 1×10^5 ml^{-1} in serum-free differentiation (SF-D) media[27] and cultured on an orbital shaker at 70 rpm for ~18 hrs in the absence of growth factors to form EBs. At D2, EBs were split 1:3 in SF-D media containing recombinant human (rh) VEGF (5 ng ml^{-1}; R&D Systems), rhBMP4 (10 ng ml^{-1}; R&D Systems) and Activin A (5 ng ml^{-1}; R&D Systems) for 48 hr. At D4, EBs were split 1:1 or 1:2 in SF-D media containing rhVEGF (5 ng ml^{-1}; R&D Systems), rhBMP4 (10 ng ml^{-1}; R&D Systems) and Activin A (5 ng ml^{-1}; R&D Systems) for 24 hr. For bulk cultures, EBs were washed at D5 and D6 and cultured in SF-D media containing rhVEGF (5 ng ml^{-1}; R&D Systems) and SCF (50 ng ml^{-1}; BioLegend). From D4 onwards EBs were grown in petri dishes coated with 5% (v/v) Poly-heme solution (Sigma, Cat# P3932-10G). For EHT cultures, D5 EBs were dissociated with Trypsin-LE (Gibco), stained with anti-Flk-1 (APC) antibody (Supplementary Table 3) for 30 min on ice and Flk-1$^+$ cells isolated by MACS using anti-APC microbeads (Miltenyi, Cat# 130-090-855) were plated on Matrigel (Corning, Cat# 354230) coated 96 or 12 well plates at a concentration of 5×10^4 cells/200 μl in SF-D containing rhVEGF (5 ng ml^{-1}; R&D Systems), rhbFGF (10 ng ml^{-1}; R&D Systems) and SCF (50 ng ml^{-1}; BioLegend) to form HE for 72 hours. Media was changed on D6 and D7. For Runx1 induction 90 ng/mL and 300 ng/mL of doxycycline, dissolved in water, was added to the culture media from day 6-8.

Hematopoietic progenitor colony assays

EBs/EHT monolayers were dissociated at D5, D6 or D8 and 5×10^4, 2×10^4 or $1 \times 10^5/2.5 \times 10^4$ cells, respectively, were plated in Methylcellulose-Based Medium (MethoCult GF M3434; Stem Cell Technologies). Primitive erythroid colonies were counted at day 5 and definitive erythroid, granulocyte/macrophage and mixed colonies counted at 7-8 days post-plating. For all statistical analyses unpaired two-tailed Student's t-tests were performed in GraphPad Prism 8 (version 8.1.0).

Flow cytometry, cell sorting and MACS

EBs were dissociated using Trypsin-LE. For EHT cultures floating and adherent cells were pooled, washed 3x with FACS buffer (PBS + 2% FCS), stained with antibodies for 30 min (4°C), washed and resuspended in FACS buffer containing DAPI (1:5000, BD Pharmigen) and analysed on either a BD Fortessa X20 or a Cytek DxP8. Cell sorting for RNA-Seq and ATAC-Seq was completed on a MoFlo Astrios. For MACS, cells were stained at a concentration of 10^7 cells/150 uL FACS buffer containing 3.75 uL of anti-Flk-1(APC)

antibody for 30 min (4°C), washed with PBE (PBS + 2mM EDTA + 0.5% BSA) and incubated in 80 uL of PBE + 20 uL of anti-APC microbeads (Miltenyi, Cat# 130-090-855) for 30 min (4°C), washed with PBE then passed over a LS magnetic column twice. For intracellular flow cytometry day 3-5 EoV5/V5 EBs were dissociated and stained for Flk-1 and PdgfRa prior to fixation. Cells were subsequently permeabilized and V5 staining was performed using the FoxP3 Staining Buffer Set (Invitrogen, Cat# 00-5523). Antibodies used are listed in Supplementary Table 3. The flow cytometry data was collected using BDFacsDiva (version 8), FlowJoCE (version 7.5) or Summit (version 6.3.1) software. For all statistical analyses unpaired two-tailed Student's t-tests were performed in GraphPad Prism 8 (version 8.1.0).

RNA isolation and quantitative RT-PCR

Total RNA was isolated using the RNeasy Mini Kit (QIAGEN, Cat#74104) using on-column DNase treatment. Complementary DNA was generated using the SuperScriptIII kit (Invitrogen) with oligo-dT primers. RT–qPCR was performed using the Quantitect SYBRGreen PCR kit and a Rotor-gene Q (Qiagen) and analysed using the delta-delta Ct method, as described previously[35]. Primer sequences are provided in Supplementary Table 2.

RNA-Seq

RNA isolated from Flk-1^{hi}/PdgfRa^{-} single cell suspensions (1.5x10^{5} cells) from three independent hematopoietic differentiations of WT (CCE) and Eomes-null (clone 6A6, CCE) cells using the RNeasy Micro Kit (QIAGEN, Cat#74004) was normalized to 800ng per sample, depleted of cytoplasmic and mitochondrial ribosomal RNA sequences (Ribo-Zero Gold rRNA Removal Kit (H/M/R), Cat: #MRZG12324) and library preparation performed using the Illumina TruSeq Stranded Total RNA Library Prep (H/M/R) (Cat: #20020597), followed by sequencing (75-cycle paired end) on the Illumina HiSeq4000 platform.

RNA-Seq analysis

Paired-end reads were aligned against the mm10 genome using the STAR RNA-seq aligner with default parameters outputting bam files using --outSAMtype BAM SortedByCoordinate[64]. BAM file primary alignments with a mapping quality of > 254 were treated as RNA-Seq data and imported into Seqmonk 1.45.4.

(https://www.bioinformatics.babraham.ac.uk/projects/download.html#seqmonk). The RNA-Seq quantitation pipeline (p<0.05 and multiple testing correction applied) in SeqMonk utilizing DESeq2[65] was performed to identify significantly differentially expressed genes (p<0.05, fold change > 1.5 and FPKM >1).

scRNA-Seq

10,000 Flk-1^{hi}/PdgfRa^{-} cells from D4/5 WT and Eomes-null EBs were sorted (BD FACSAria III) into 20 μL PBS/0.05% BSA (non-acetylated) and the volume topped up to 38 μL for loading onto the 10X Chromium Controller. Processing of samples was performed using the Chromium Single Cell 3' library & Gel Bead Kit v3 (10x Genomics). Barcoded

cell cDNAs were pooled and converted to sequence ready libraries. Multiplexed libraries were then sequenced on Illumina Nextseq using a high output 150bp Nextseq V2.5 kit.

scRNA-Seq analysis

Sequencing data was demultiplexed in the binary base call (BCL) format, FASTQ files were aligned to the mm10 genome using 10X Genomics Cell Ranger software (version 2.0.0) and unique molecular identifier (UMI) counts determined. The Seurat v3 software package[54, 66] was used in R Studio to perform scRNA-Seq analysis. Pre-processing was performed and cells with > 2000 RNA features and < 8 % mitochondrial RNA were used for downstream analysis. Each sample was randomly down sampled to include 3805 cells and WT and Eomes-null samples from days 4 and 5 were merged together, normalized and 2000 variable features were identified using the VST method. Integration anchors for WT and Eomes-null Seurat objects were identified and integration was performed using the first 20 principle component (PC) dimensions. Clusters were identified and UMAPs generated using the first 16 PC and a resolution of 0.8. Cell type identities were assigned by comparing the conserved markers from each of the 13 clusters to cell type markers previously published for cell types identified in E6.5 to E8.5 mouse embryos[15]. Supplementary Table 1 lists the conserved markers.

In vitro cell type annotation was performed by mapping against the mouse gastrulation atlas[15]. Raw counts from both experiments were merged and normalised using the scater (1.14.6) package[67]. Then, highly variable genes were extracted from the joint data using scran's (1.14.6) decomposeVar function[68]. Genes with an FDR lower than 0.05 were considered as highly variable and used to compute the top fifty principal components along the joint dataset. Batch correction was performed on the gastrulation atlas principal components using the fastMNN's algorithm following the exact procedure from the original publication[15]. Integrated datasets were also corrected using fastMNN. *In vitro* cells were annotated by looking at the top 35 nearest neighbours from the atlas and selecting the most frequent cell type. A mapping score was assigned to reflect the mapped cell type frequency, where a higher score indicates a more consistent annotation. *In vitro* cells were additionally mapped back onto the force directed graph of hematoendothelial cells (hematoendothelial differentiation trajectory) from the original publication[15] by identifying the single nearest neighbour.

ATAC-seq

Tagmentation and indexing of single cell suspensions ($6x10^4$ cells) from three independent differentiations of WT (CCE) and Eomes-null (clone 6A6, CCE) day 4 Flk-1^{hi}/PdgfRa$^-$ cells was performed as previously described[38]. To control for sequence bias of the Tn5 transposase, 100ng genomic DNA of WT (CCE) ESCs was also tagmented and indexed. Libraries were purified with two rounds of Agencourt AMPure XP bead cleanup (Agencourt, 1.5× bead:sample ratio). Library size and concentration were determined using the 2100 Bioanalyzer High Sensitivity DNA Kit (Agilent). Samples were sequenced using a 75-cycle paired end Nextera kit with custom Nextera index primers taken from Table S1 in Buenrostro et al. 2013[38] on the Illumina HiSeq4000 platform.

ATAC-seq analysis

Paired-end reads were aligned to the mouse genome assembly mm10 using Bowtie2[69] with the very-sensitive option, sorted and mitochondrial reads discarded using Samtools[70] and duplicates removed using Picard (https://broadinstitute.github.io/picard/). Bigwig files were generated using deepTools2[71]. Biological replicates were randomly downsampled to contain the same number of reads for each individual sample and peaks in each sample called using MACS2[72] using the Tn5 control as a control. MACS2 called peaks with a p-value $< 10^{-3}$ were used in downstream analyses. Significant changes in ATAC-Seq datasets were identified using the DiffBind package (version 2.2.12) (http://bioconductor.org/packages/release/bioc/html/DiffBind.html) using bam files and an integrative bed file of all identified peaks in each sample with the following filters: FDR < 0.05, fold change > 1.5. GREAT 4.0.4 analysis[73] was performed using default basal plus extension parameters with whole genome as a background to identify peak-gene associations. Enrichment of TF motifs in differentially accessible ATAC-seq peaks was performed using the Analysis of Motif Enrichment (AME 4.12.0) feature in the MEME suite[74] with a background control of all ATAC-seq peaks.

Bigwig files were downloaded from GSE47085 and genomic coordinates were converted from mm9 to mm10 using Crossmap 0.2.9[75]. An SCL peak file was downloaded from Supplementary Table S1A from Van Handel et al. 2015[39] and genomic coordinates were converted from mm9 to mm10 using UCSC LiftOver. Bedtools was used to intersect peak files and identify overlapping genomic regions[76]. GREAT 4.0.4 analysis[73] was performed using default basal plus extension parameters with whole genome as a background to identify peak-gene association. Identified genes were annotated in Seqmonk 1.45.4 for comparison of ATAC-Seq and gene expression changes from RNA-Seq. Changes in ATAC-Seq signal were assessed using heatmaps generated in deepTools2[71], and genomic snapshots visualized in IGV[77] generated from bigwig files creates using deepTools2[71].

CRISPR modification of ESCs

Custom synthetic crRNA (using the CC-Top CRISPR design tool[78]) and ssODNs (Integrated DNA Technologies, USA) were resuspended in IDT duplex buffer. Sequences are provided in Supplementary Table 5. Cas9 ribonucleoprotein (RNP) complexes were assembled immediately prior to electroporation following the manufacturer's protocol (Alt-R CRISPR-Cas9 System:Delivery of ribonucleoprotein complexes into Jurkat T cells using the Neon® Transfection System). ESC were electroporated using the Neon transfection system (Voltage = 1600V, pulse width = 10 ms, number of pulses = 3) with the appropriate ssODN (50 pmol) and RNP. If two crRNAs were used then RNPs were produced separately and mixed 1:1 prior to electroporation.

For generation of Eomes-null Runx1-Venus and Eomes-null SCL-Cherry reporter and Eomes-null iRunx1 ESCs two custom crRNAs (Supplementary Table 6) were designed to recapitulate the previously described Eomes loss of function allele[23]. ssODNs were designed that contained a 5' homology arm upstream of the intron 1 DNA DS break site, followed by insertion of a new EcoRV, Sph1 or Spe1 restriction site and a 3' homology arm located downstream of the intron 5 DNA break site (Supplementary Table 6). 10 uL of 2×10^4 ESCs

in Buffer R were electroporated with 1 uL of a 1:1 mix of the RNPs and 2 uL of the ssODN. Low density plating was performed after 72 hrs, and after 7-10 days clones were picked and screened using a three primer PCR strategy that simultaneously amplified the WT allele and the null allele (Supplementary Table 2). Genotypes of clones were verified using Southern blotting or PCR followed by restriction enzyme digests.

For generation of the Eomes$^{V5/V5}$ ESC lines a custom crRNA was designed to target the UAG translational stop site in exon 6 of Eomes and a ssODN was designed to insert a triple glycine V5 epitope tag (3XGly-V5) directly upstream of the UAG translational stop site of Eomes (Supplementary Table 6). Homozygous insertion of the 3XGly-V5 tag at the C-terminus of the Eomes locus was assessed by PCR across the C-terminus of Eomes with primers listed in Supplementary Table 2. In frame insertion with the correct 3XGly-V5 sequence was confirmed via Sanger sequencing of a 971 bp PCR product (Supplementary Table 2) that spanned the C-terminus of Eomes. Western blotting and immunofluorescence staining were performed on day 4 EBs to confirm successful V5 tagging of the endogenous Eomes protein.

Generation of the Runx1-Venus ESC reporter line

For generation of the Runx1-Venus mouse ESC reporter line a 3xFlag-P2A-Venus was inserted in the last exon of Runx1 (exon 6), before the stop codon. Briefly, a 4kb 5' homology arm and a 4.2 3' homology arm were amplified from E14 gDNA by PCR and cloned into pUC19 (Invitrogen). A GeneARt (Invitrogen) synthetic construct consisting of Runx1_ex6-3xFlag-P2A-Venus was cloned into the pUC19 vector containing the homology arms using Gibson assembly (pUC19-Runx1-Venus_GA_FP: ccaacatgcccccccgCGCGCCTGGAGGAGGCCG, pUC19-Runx1-Venus_GA_RP: cggcaggcccagtccCTCGATGGCGATGGCGCTC). The resulting pUC19-Runx1_Ex6-P2A-Venus-Long HAconstruct was used for transfection into undifferentiated E14 ESCs with a CRISPR/Cas9 vector expressing a gRNA (Supplementary Table 5) that cut immediately preceding the RUNX1 stop codon. The guide RNA (gRNA) was designed using the MIT CRISPR design tool (http://crispr.mit.edu/)[79]. The double stranded gRNA was constructed by annealing oligos (Integrated DNA Technologies; IDT) consisting of the gRNA sequence (forward) and reverse complement sequences (reverse) (Supplementary Table 5). The gRNA was cloned into the BbsI site of pX458 (Addgene plasmid 48138); BbsI restriction sites were added to the oligos for this purpose. All constructs were verified by Sanger sequencing. E14 ESCs were transfected using TransIT LT1 (Mirus) and a pX458:pUC19 ratio of 1:2. Integration was checked by long-range PCR with a forward primer outside of the 5' HA and a reverse primer 3' of the Runx1 endogenous stop codon, generating a 5.8kb amplicon for the correctly targeted allele and a 4.4kb amplicon for the wild type allele (Supplementary Table 2). A clone with the Venus reporter integrated in both alleles (RV11) was used for all experiments.

ChIP-Seq

Day 4 Eomes$^{V5/V5}$ (CCE) and WT (CCE) D4 EBs were dissociated and ~3-4x10^7 cells were cross-linked for 10 min at RT with 1% (v/v) formaldehyde, and quenched with 125mM glycine. Nuclei were recovered and lysed to obtain chromatin, which was then sonicated to

200–500 bp, pre-cleared with protein G Dynabeads (Thermofisher Scientific) and ~175 ug of chromatin was immunoprecipitated with 10μg of anti-V5 (Abcam cat# ab9116, lot# GR: 322448-4) bound to protein G Dynabeads overnight on a rotator at 4°C. Dynabeads were washed and immune complexes were eluted in IP elution buffer (1% SDS, 0.1M NaHCO3), reverse crosslinked overnight at 65°C, RNaseA treated for 1.5hrs at 42°C, proteinase K treated for 2hrs at 45°C and DNA was recovered using a Zymo column kit. DNA was multiplexed and paired end sequencing was performed on a single lane of an Illumina HiSeq4000 platform.

ChIP-Seq analysis

Paired-end reads were aligned to the mouse genome assembly mm10 using Bowtie2[69] with default parameters. PCR duplicates were removed using Samtools 1.9[70]. Peaks were called against input DNA using MACS 2.1.2[72] and were considered significant if they had a fold enrichment > 2 and FDR < 0.05. Bedtools 2.27.1[76] was used to intersect the peak files from both Eomes[V5/V5] clones and subtract peaks called in the WT control and genomic intervals located in mm10 blacklist regions (https://www.encodeproject.org/files/ENCFF547MET/@@download/ENCFF547MET.bed.gz), generating a peak file containing 338 genomic intervals used for downstream analyses (Supplementary Table 6). The HOMER (v4.10.4) software package[80] was used to perform motif enrichment analysis. GREAT 4.0.4 analysis[73] was performed using default basal plus extension parameters with the whole genome used as a control to identify peak-gene associations. Heatmaps and bigwig files were generated using Deeptools 3.1.3[71]. Bigwig files and peak files were downloaded from GSE69101[49]. Data from GSE110164[50] were downloaded and used to generate peak files and bigwig files as previously described[81]. Bigwig files and peak files were downloaded from GSE128466[51].

Statistics and Reproducibility

Embryos were imaged and/or stained and genotyped retrospectively to exclude any bias. The sample size (*n*) for each experiment is described in the corresponding figure legend, and all experiments were conducted with at least three biological replicates unless otherwise stated. All statistical analyses were performed using GraphPad Prism (8.1.0) except for sequencing data analyses. Quantitative data displayed as bar charts indicate the mean ± SEM (represented as error bars) and individual replicates are shown as dots. Two-tailed unpaired Student's t-tests were used for pairwise comparisons between groups. Statistical significance values (*P*) are shown directly within the figure above pairwise comparisons.

Extended Data

a E6.5 - Mid Streak   **b** E7.5 - Late Streak

Flk-1   Flk-1   2.5X
Eomes   Eomes   2.5X
Merge   Merge   2.5X
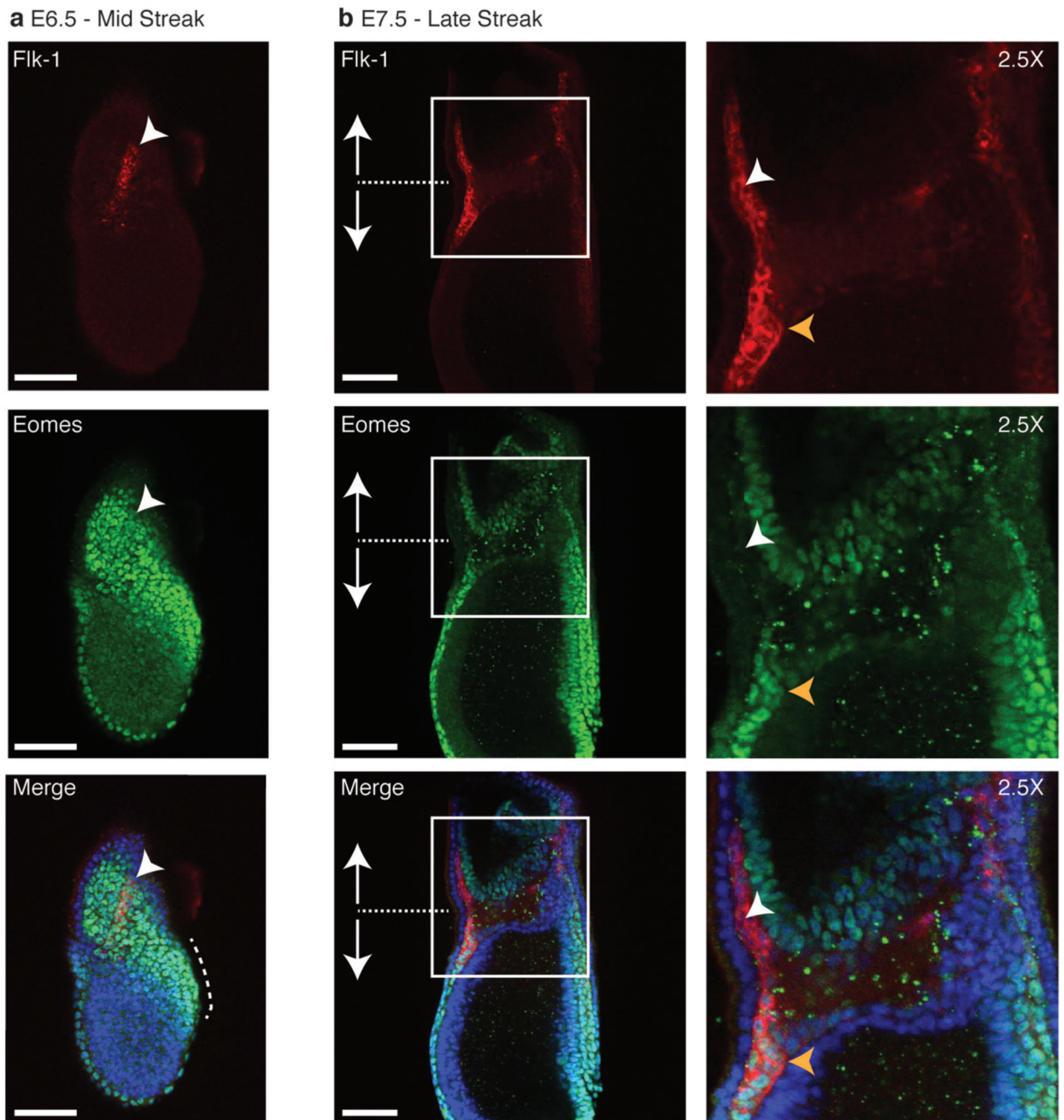
Extended Data Fig. 1. Eomes and Flk-1 expression at the outset of mouse gastrulation.
a,b,Immunofluorescence staining of E6.5(**a**) and E7.5 (**b**) wildtype embryos for Flk-1 (red)
and Eomes (green); Images representative of 5 embryos (E6.5) and 8 embryos (E7.5). Nuclei
are stained with DAPI (blue). Dotted white lines indicate the extraembryonic/embryonic
boundary. White boxes denote the zoomed in areas displayed in the far-right panel. White

arrows indicate Flk-1+ extra-embryonic mesodermal cells. Orange arrows indicate Flk-1+ embryonic mesodermal cells. Scale bars, 100 μM.
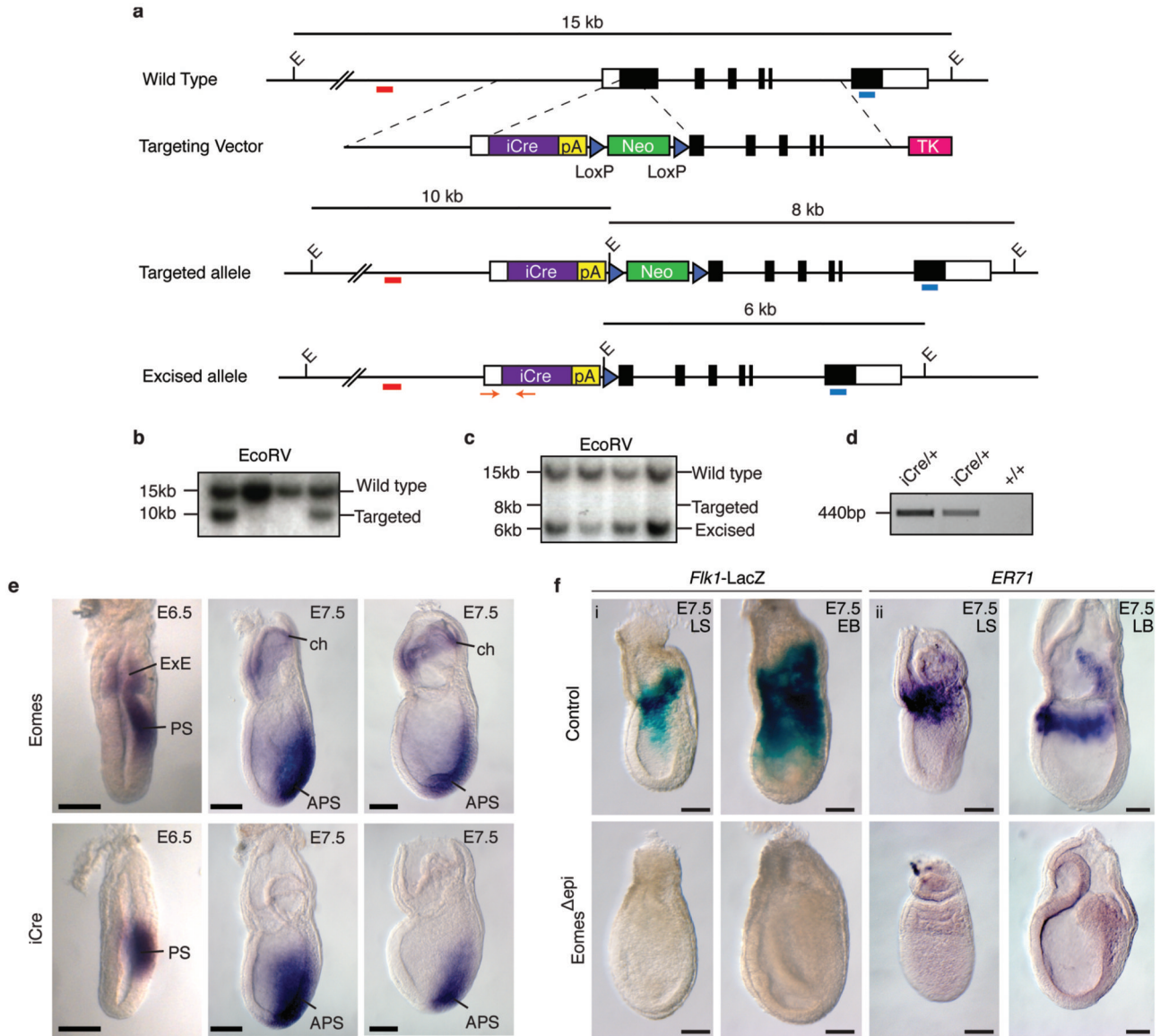
Extended Data Fig. 2. Generation of the Eomes^iCre allele.

Targeting strategy used to generate the Eomes^iCre allele. The targeting vector introduces a mammalian codon-improved Cre (iCre), β-globin polyA cassette into the endogenous Eomes initiator methionine and a LoxP flanked PGK-Neo positive drug selection cassette and TK negative selection cassette. Red and blue lines indicate the locations of 5' external (red) and 3' external probes (blue, exon 6) used for Southern blotting. Orange arrows indicate the location of primers used for PCR genotyping. E = EcoRV. **b,** Southern blot showing wildtype (15kb) and targeted (10kb) alleles. (Red probe) **c,** Southern blot after Cre-mediated excision of the Neo drug selection cassette showing excised targeted (6kb) and wild type (15kb) alleles and loss of the targeted allele (8kb). (Blue probe) **d,** PCR

genotyping of Eomes^{iCre} mice; iCre band size is 440bp. (b-d) Southern blots and PCR genotyping blots are representative of at least 3 independent experiments. **e,** Wholemount in-situ hybridization (WISH) comparing Eomes and iCre expression in Eomes$^{iCre/+}$ embryos. ExE, extra-embryonic ectoderm; ch, chorion; PS, primitive streak; APS, anterior primitive streak. Scale bars, 100μM **f,** Evaluating the expression of extra-embryonic mesodermal markers upon Eomes conditional inactivation from the epiblast (Eomes ^{epi}). (**i**) Wholemount X-gal staining of E7.5 control (top) and mutant Eomes ^{epi} (bottom) embryos carrying a Flk-1-LacZ reporter allele. (**ii**) WISH analysis of ER71 expression in control (top) and mutant Eomes ^{epi} (bottom) embryos. Scale bars, 100μm. LS, late streak; EB, early allantoic bud stage. (e-f) Images are representative of at least 3 embryos from each gestational stage and genotype.
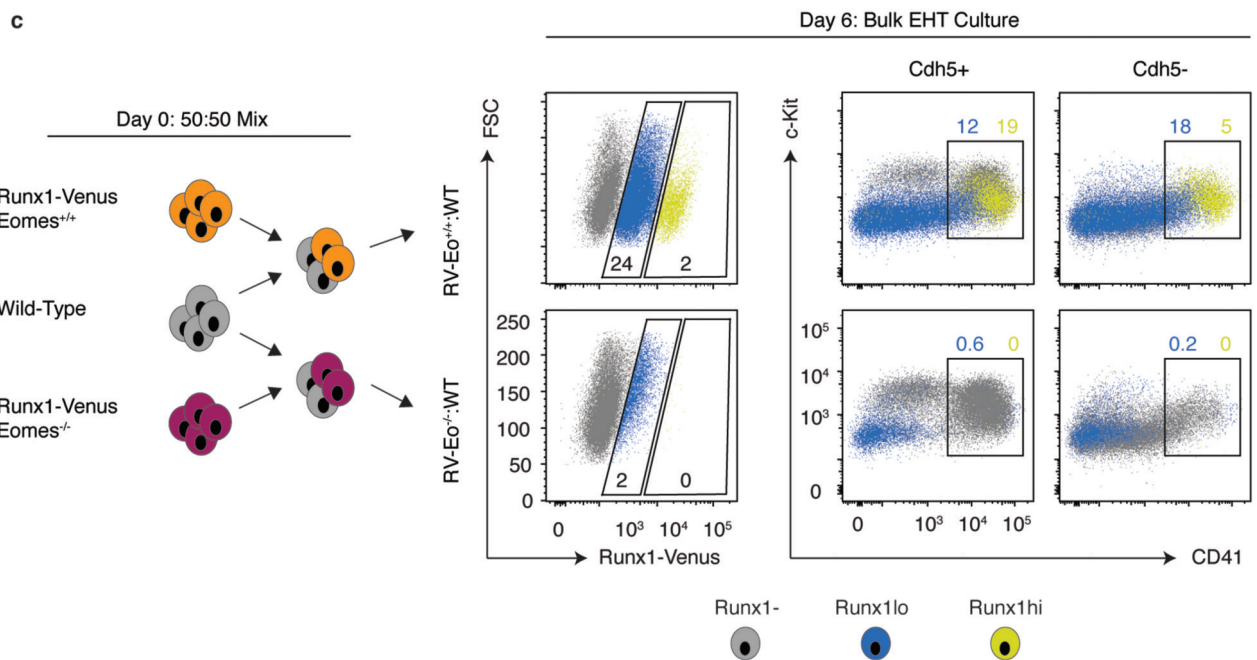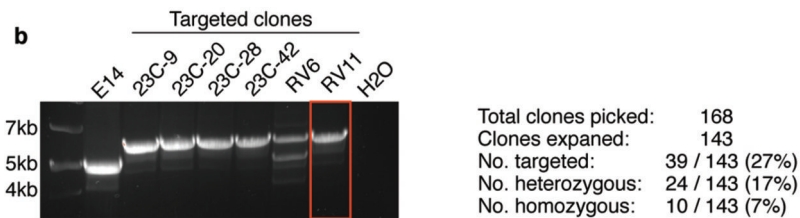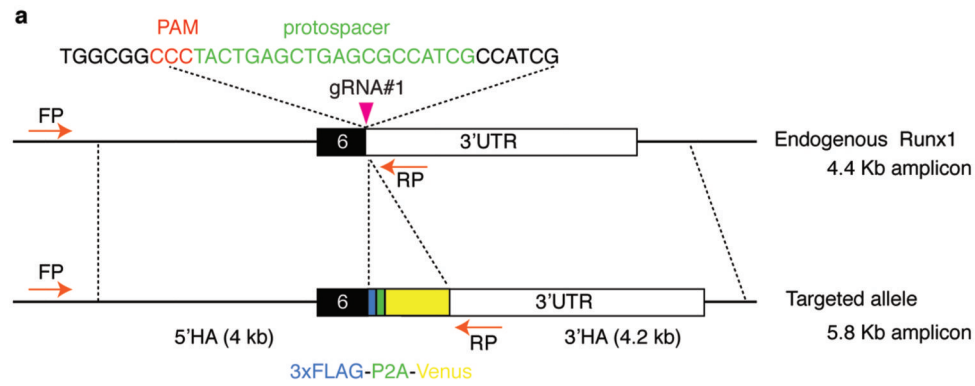
Extended Data Fig. 3. Generation of the Runx1-Venus ESC reporter line.
a, Targeting strategy used to generate the Runx1-Venus allele. A 3xFlag-P2A-Venus was inserted in the last exon of Runx1 (exon 6), before the stop codon. Pink arrow indicates the locations of Cas9-gRNA induced DNA double stand break immediately preceding the Runx1 stop codon. Orange arrows indicate locations of primers used for PCR genotyping **b,** Integration of the targeting vector was confirmed using long-range PCR; Runx-1Venus band size is 5.8kb, WT band size is 4.4kb.

A clone with the Venus reporter integrated in both alleles (RV11 - red box) was used for all experiments. This experiment was performed once. **c,** Assessing Eomes' requirement for cell autonomous Runx1 expression during hematopoiesis (left panel). At day 0 WT (grey) cells were mixed in equal proportions with either $Eo^{+/+}$ Runx1-Venus ESCs (orange) or $Eo^{-/-}$ Runx1-Venus ESCs (purple). Flow cytometric analysis was performed on bulk EHT RV-Eo$^{+/+}$:WT (top) and RV-Eo$^{-/-}$:WT co-cultures at day 6 to assess Runx1-venus, cKit and CD41 expression. Runx1-venus was expressed at varying levels (left flow cytometry panel); Runx1-negative, grey dots; Runx1-lo, blue dots; Runx1+, yellow dots. Percentages of Runx1-Venus^{lo} (blue) and Runx1-Venus^{+} (yellow) cells within the CD41^{hi} cell population are indicated by coloured numbers in the middle and right flow cytometry panels; Representative of 1 Runx-1 Venus Eomes$^{+/+}$ and 2 Runx1-Venus Eomes$^{-/-}$ clones.
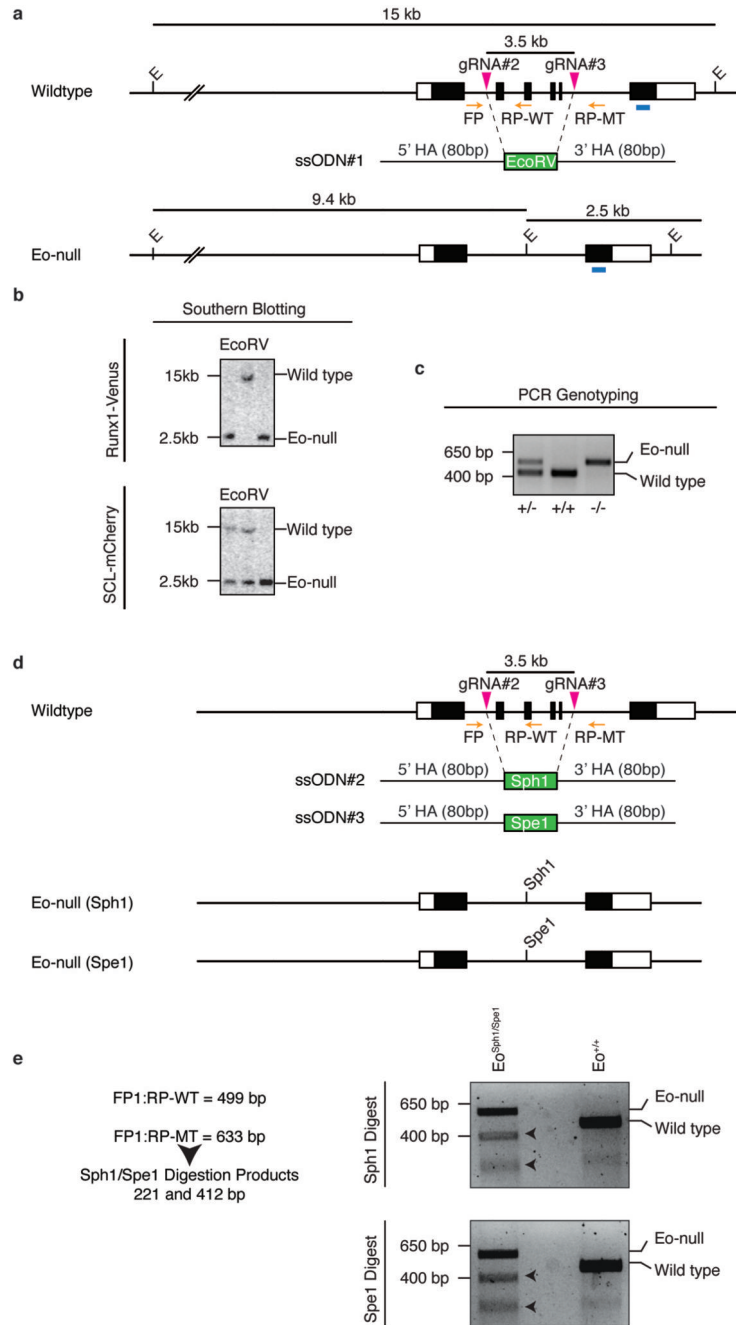
Extended Data Fig. 4. Re-generation of the Eomes loss-of-function allele in the SCL-mCherry and Runx1-Venus ESC reporter lines and the iRunx1 Runx1-/- ESC using CRISPR-Cas9.
a, The targeting strategy used to re-generate the Eomes-loss of function allele[23] in SCL-mCherry and Runx1-Venus ESC reporter lines. An ssODN was used to patch an EcoRV site in between introns 1 and 5 to delete a 3.5 kb region, including exons 2-5 of the Eomes locus. Pink arrows indicate the locations of Cas9-gRNA induced DNA double strand breaks in intron 1 and intron 5. Blue lines (exon 6) indicate the location of a 3' external Southern blotting probe. Orange arrows indicate the location of primers used for PCR genotyping. E = EcoRV. **b,** Southern blots showing wild type (15kb) and targeted (2.5kb) alleles in Runx1-

Venus (top) and SCL-mCherry (bottom) ESC lines. Representative of 2 independent experiments. **c,** PCR genotyping of Eomes-null ESCs; WT band size is 401bp, Eomes-null band size is 535 bp. **d,** The targeting strategy used to re-generate the Eomes-loss of function allele in the iRunx1 Runx1$^{-/-}$ ESC line. ssODNs were used to patch an Sph1/Spe1 restriction sites in between introns 1 and 5 to delete a 3.5 kb region, including exons 2-5 of the Eomes locus. Pink arrows indicate the locations of Cas9-gRNA induced DNA double strand breaks in intron 1 and intron 5. Orange arrows indicate the location of primers used for PCR genotyping. **e,** PCR genotyping of Eomes-null ESCs; WT band size is 499 bp, Eomes-null band size is 633 bp and digestion products of the Eomes-null PCR product are 221 bp and 412 bp. iRunx1 Runx1$^{-/-}$ Eomes$^{-/-}$ clones had insertion of both Sph1 and Spe1 restriction sites, indicating a homozygous deletion. Representative of 2 independent experiments.
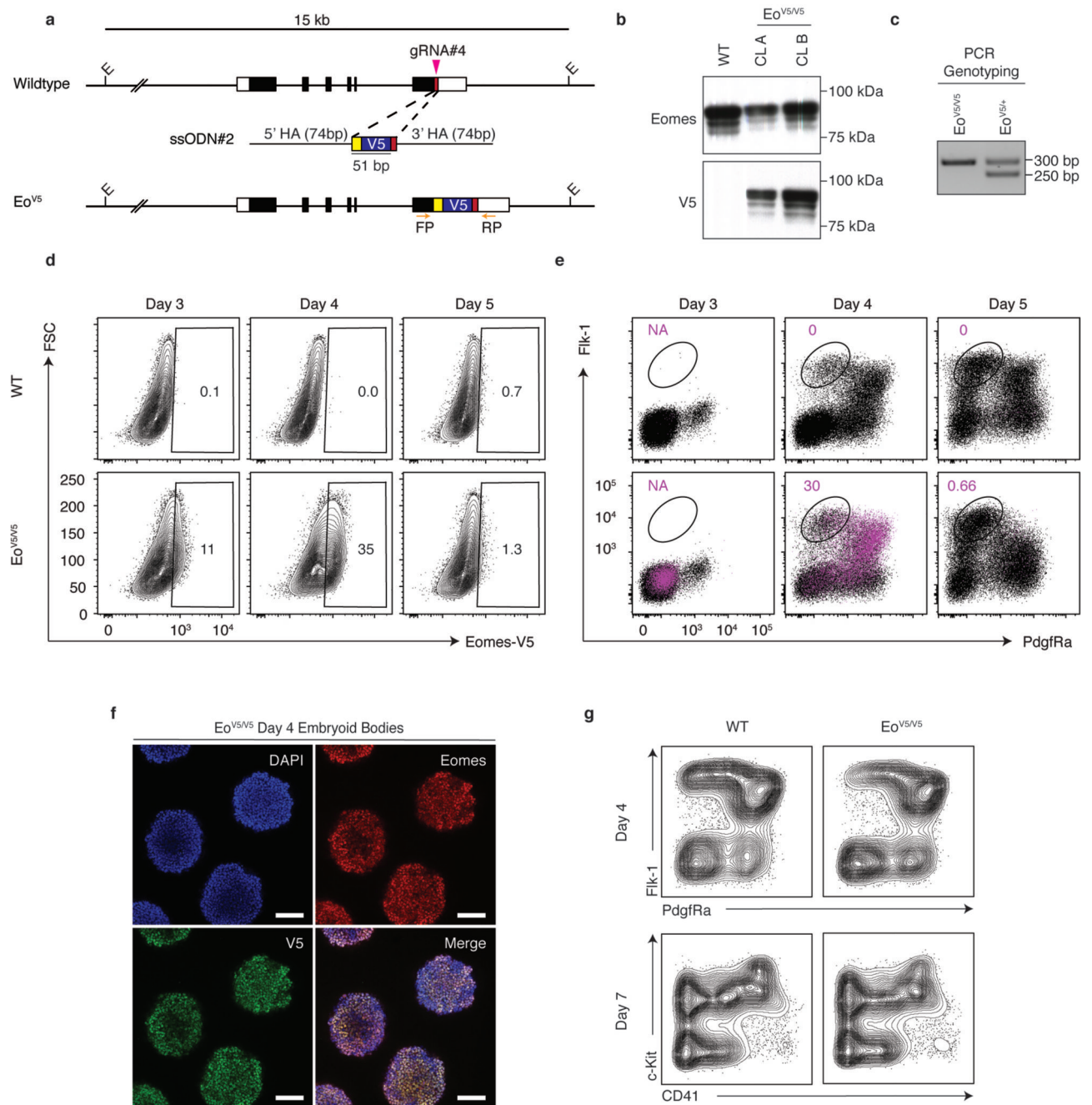
Extended Data Fig. 5. Generation of the Eomes$^{V5/V5}$ ESC line for ChIP-Seq.
a, The targeting strategy used to insert a 3XGly-V5 tag directly upstream of the UAG translational stop codon (exon 6) at the C-terminus of the Eomes locus using an ssODN. The pink arrow indicates the location of the Cas9-gRNA induced DNA double strand break. Orange arrows indicate the location of primers used for PCR genotyping. **b,** Western blotting of whole cell protein lysates from Eo$^{V5/V5}$ and WT day 4 EBs shows that the three isoforms of Eomes protein (upper panel) are V5 tagged (lower panel) in both Eo$^{V5/V5}$ clones. This experiment was performed once. **c,** PCR genotyping of Eomes-V5 targeted clones; WT band

size is 250bp, Eo-V5 band size is 301 bp. Representative of at least 3 independent experiments. **d, e,** V5 protein expression was evaluated in day 3-5 Eomes$^{V5/V5}$ EBs using intracellular flow cytometry. **d** Equivalent stage WT EBs were used as a gating control (upper panel). **e,** Additionally, EBs were stained for Flk-1 and PdgfRa expression; purple dots indicate cells that are V5+ and numbers indicate the proportion of cells in the Flk-1^{hi}/ PdgfRa^{-} that are V5^{+}; Representative of 1 wildtype and 2 Eo$^{V5/V5}$ clones. **f,** Representative immunofluorescence staining of Eo$^{V5/V5}$ day 4 EBs for Eomes (red) and V5 (green); 2 biologically independent samples. Nuclei are counter stained with DAPI (blue). Scale bars, 100 μM. **g,** Representative flow cytometric analysis of Flk-1/PdgfRa (top) and CD41/c-Kit (bottom) expression in WT (left) and Eo$^{V5/V5}$ (right) day 4 and day 7 EBs, respectively; Representative of1 WT and 2 Eo$^{V5/V5}$ clones
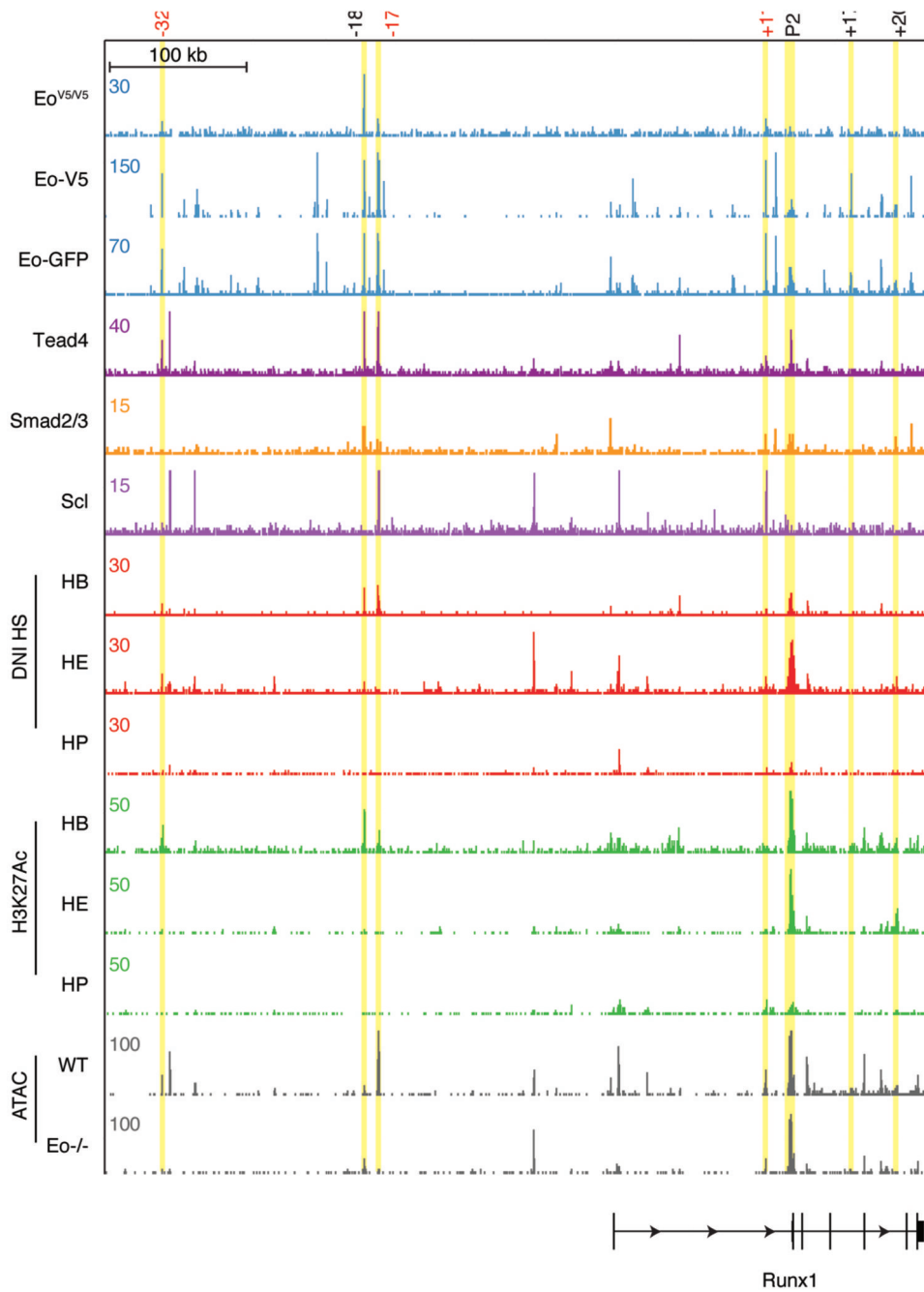
Extended Data Fig. 6. Eomes binds multiple Runx1 cis-regulatory regions.
IGV snapshots of Eomes$^{V5/V5}$, Eomes-V5/ Eomes-GFP[51], Tead4[49], Smad2/3[50] and Scl[39]
ChIP-Seq peaks. H3K27Ac ChIP-Seq peaks and DNase1 hypersensitivity (DN1 HS) at
different stages of hematopoietic development *in vitro*; HB, hemangioblast (T$^+$/Flk-1$^+$); HE,
hemogenic endothelium (Tie2$^+$/Kit$^+$); HP, hematopoietic progenitor (CD41$^+$)[49]. Yellow bars
highlight Eomes bound sites identified in the Eomes-V5 dataset[51]. The numbers above
coloured columns indicate the relative location of these sites in kilobases to the TSS at P1 of

the Runx1 locus. Red numbers indicate sites which have reduced chromatin accessibility in Eomes-/- Flk-1^{hi}/PdgfRa$^-$ cells. P1, promoter 1; P2, promoter 2.
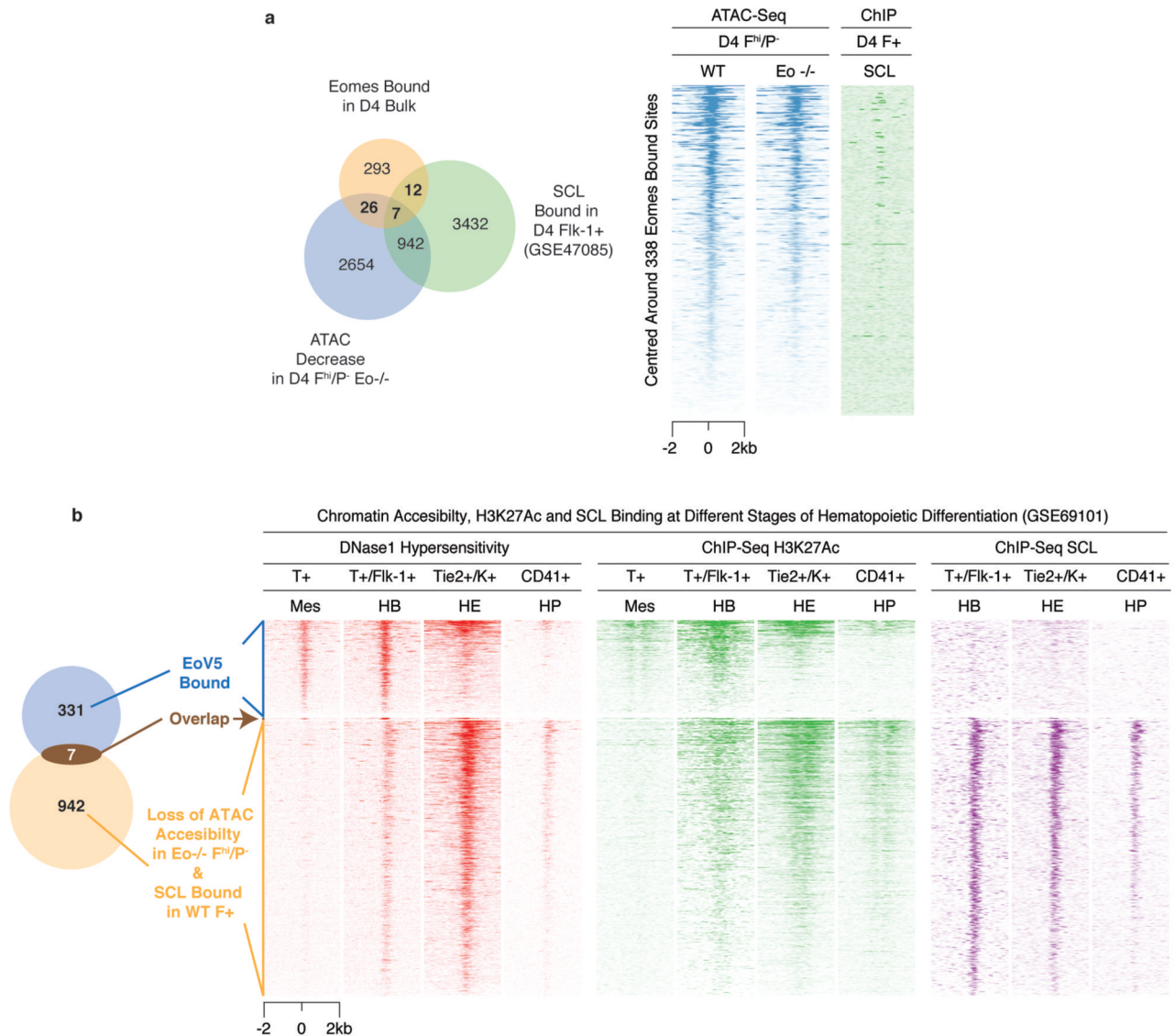
Extended Data Fig. 7. Comparing Eomes bound ChIP-Seq peaks with the subset of ATAC-Seq peaks that are Eomes-dependent and normally bound by SCL at various stages of hematopoietic differentiation.

a, Venn diagram depicting the overlap of Eo-V5 ChIP-Seq peaks in D4 EBs, SCL ChIP-Seq peaks in D4 Flk-1$^+$ EBs[39] and sites of reduced chromatin accessibility in day 4 Eo$^{-/-}$ Flk-1$^+$/ PdgfRa$^-$ cells. Heatmaps showing ATAC signals (blue) from WT or Eomes$^{-/-}$ day 4 Flk-1^{hi}/ PdgfRa$^-$ cells and SCL ChIP-Seq signal (green) from day 4 WT Flk-1$^+$ cells[39]. All heatmaps show a 4kb region flanking peak centres of the 338 Eomes bound sites. **b,** Venn diagram depicting the overlap of Eo-V5 ChIP-Seq peaks in D4 EBs with sites of reduced chromatin accessibility in day 4 Eo$^{-/-}$ Flk-1^{hi}/PdgfRa$^-$ cells that are normally bound by SCL in WT day 4 Flk-1$^+$ cells[39]. Heatmaps show DNAseI hypersensitivity signal (red), ChIP-Seq signal for

H3K27Ac (green) histone modifications and SCL occupancy (purple) in different cell populations that develop during hematopoietic differentiation. Mes, mesoderm (T$^+$/Flk-1$^-$); HB, hemangioblast (T$^+$/Flk-1$^+$); HE, hemogenic endothelium (Tie2$^+$/Kit$^+$); HP, hematopoietic progenitor (CD41$^+$)[49]. All heatmaps show 4kb regions flanking peak the peak regions indicated in the Venn diagram.
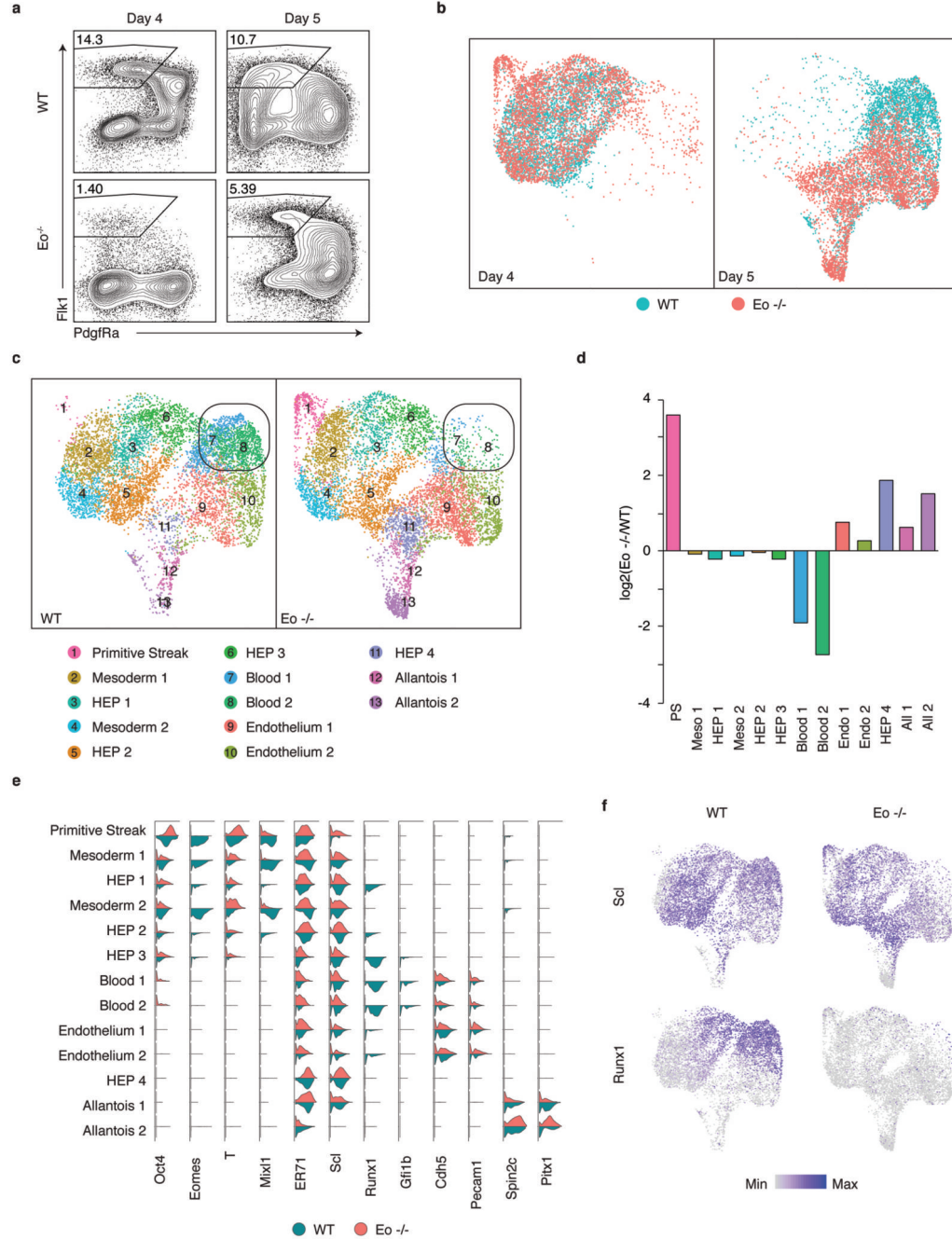
Extended Data Fig. 8. scRNA-Seq shows that hematoendothelial progenitor and endothelial subsets are still specified in the absence of Eomes function.

a, Gating strategy used to sort Flk1^{hi}/PdgfRa$^-$ cells from day 4 and day 5 wildtype and Eomes$^{-/-}$ EBs for 10X scRNA-Seq. **b, c,** Uniform manifold approximation and projection (UMAP) plots. WT (blue) and Eomes$^{-/-}$ (red) Flk-1^{hi}/PdgfRa$^-$ cells from day 4 (left) and day 5 (right) EBs; n = 3805 cells/genotype/day. **c,** WT (left) and Eomes$^{-/-}$ (right) cells coloured by their Seurat cluster/cell type annotation denoted in the legend. The black box highlights clusters 7 and 8 that are diminished in the Eomes$^{-/-}$ cultures. **d,** Log2 fold change in the abundance of Eomes$^{-/-}$ cells with respect to WT cells in each Seurat cluster. **e,** Violin plots showing mesodermal, hematovascular and allantoic gene expression levels in WT (blue) and Eomes$^{-/-}$ (red) cells within the various Seurat clusters; n = 7610 WT cells and n = 7610 Eomes$^{-/-}$ cells. Violin plots show normalized expression values, genes are indicated on the x-axis and clusters on the y-axis. **f,** Normalized expression of Scl (top) and Runx1 (bottom) overlaid on UMAPs for all single cells collected from day 4/5 Flk^{hi}/PdgfRa$^-$ wildtype (left) or Eomes$^{-/-}$ (right) EBs. HEP, hematoendothelial progenitors; Endo, endothelium; Meso, mesoderm; PS, primitive streak.
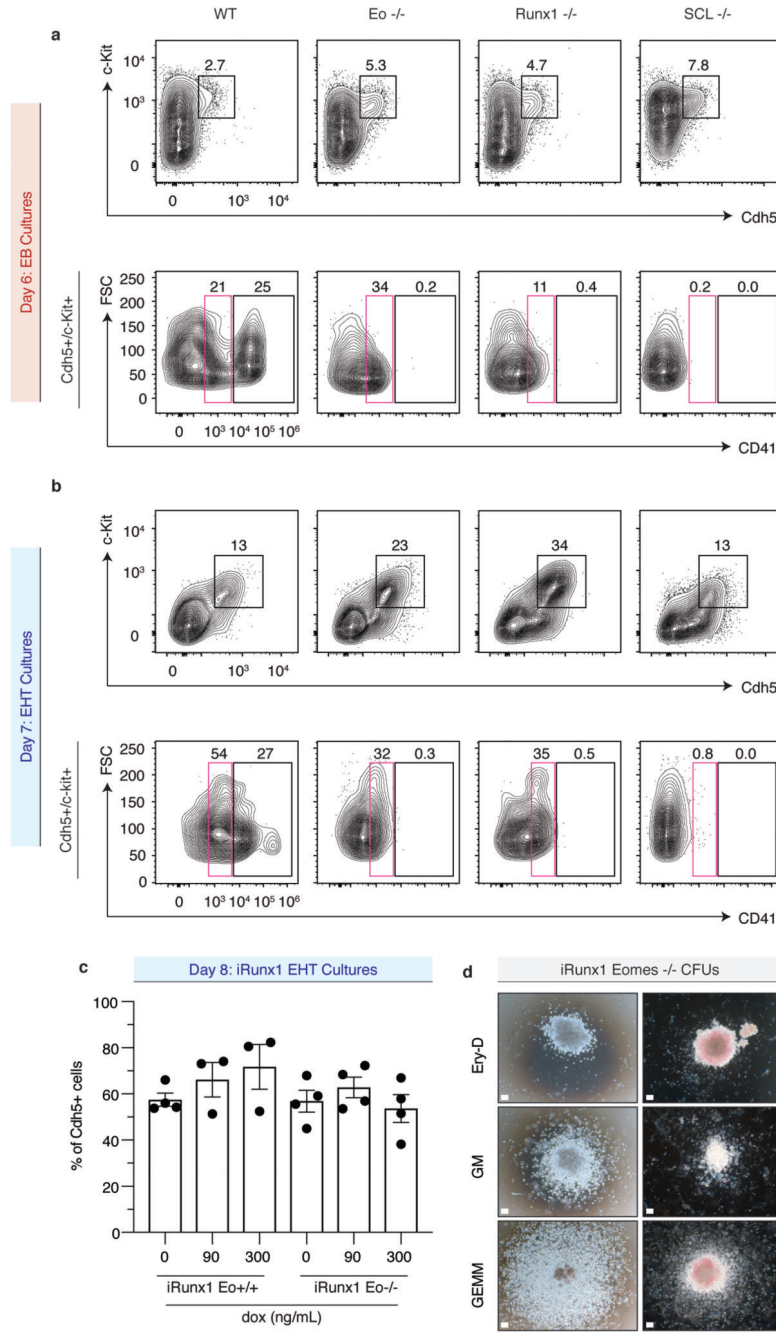
Extended Data Fig. 9. Eomes-null endothelial cells immunophenocopy Runx1-null endothelial cells.

a, b, Flow cytometric analysis of day 6 EB (**a**) and day 7 EHT (**b**) for expression of Cdh5/cKit and CD41 within the Cdh5$^+$/cKit$^+$ compartment. Pink gate highlights a CD41^{lo} subset absent in SCL-null cultures. This experiment was performed once. **c,** Proportion of Cdh5$^+$ cells in day 8 iRunx1 Eomes +/+ and iRunx1 Eomes -/- EHT cultures in which Runx1 has been uninduced (0ng/mL dox) or induced (90 and 300 ng/mL dox) from day 6-8. Graphical representations depict mean +/- SEM of n = 3 independent differentiations for iRunx1 Eo$^{+/+}$ 90ng/mL and iRunx1 Eo$^{+/+}$ 300 ng/mL and n = 4 independent differentiations for iRunx1 Eo

$^{+/+}$ 0 ng/mL, iRunx1 Eo$^{-/-}$ 0 ng/mL, iRunx1 Eo$^{-/-}$ 90 ng/mL and iRunx1 Eo$^{-/-}$ 300 ng/mL. Statistical source data are provided in Source Data Fig. 8. **d,** Representative examples of definitive erythro-myeloid colonies generated from iRunx1 Eomes$^{-/-}$ day 8 EHT cultures in which Runx1 expression was induced from day 6-8 via dox addition; 3 independent differentiations. Ery-D, definitive erythrocyte; GM, granulocyte-macrophage; GEMM, granulocyte-erythrocyte-myeloid. Scale bars, 100μM.

Supplementary Material

Refer to Web version on PubMed Central for supplementary material.

Acknowledgements

Data availability statement

The RNA-Seq, scRNA-Seq, ChIP-seq and ATAC-seq data have been deposited in the Gene Expression Omnibus (GEO) GSE140005. Previously published sequencing data that were re-analysed here are available under accession code GSE110164, GSE128466 and GSE47085. All other data supporting the findings of this study and biological materials presented in this study are available on reasonable request. Source data are available for this paper.

Code availability statement

All computational code is available from the corresponding author EJR on reasonable request.

References

1. Arnold SJ, Robertson EJ. Making a commitment: cell lineage allocation and axis patterning in the early mouse embryo. Nature reviews Molecular cell biology. 2009; 10:91–103. [PubMed: 19129791]

2. Kinder SJ, et al. The orderly allocation of mesodermal cells to the extraembryonic structures and the anteroposterior axis during gastrulation of the mouse embryo. Development. 1999; 126:4691–4701. [PubMed: 10518487]

3. Ferkowicz MJ, Yoder MC. Blood island formation: longstanding observations and modern interpretations. Exp Hematol. 2005; 33:1041–1047. [PubMed: 16140152]

4. McGrath KE, Frame JM, Palis J. Early hematopoiesis and macrophage development. Semin Immunol. 2015; 27:379–387. [PubMed: 27021646]

5. Frame JM, Fegan KH, Conway SJ, McGrath KE, Palis J. Definitive Hematopoiesis in the Yolk Sac Emerges from Wnt-Responsive Hemogenic Endothelium Independently of Circulation and Arterial Identity. Stem Cells. 2016; 34:431–444. [PubMed: 26418893]

6. Kissa K, Herbomel P. Blood stem cells emerge from aortic endothelium by a novel type of cell transition. Nature. 2010; 464:112–115. [PubMed: 20154732]

7. Boisset JC, et al. In vivo imaging of haematopoietic cells emerging from the mouse aortic endothelium. Nature. 2010; 464:116–120. [PubMed: 20154729]

8. Bertrand JY, et al. Haematopoietic stem cells derive directly from aortic endothelium during development. Nature. 2010; 464:108–111. [PubMed: 20154733]

9. McGrath KE, et al. Distinct sources of hematopoietic progenitors emerge before HSCs and provide functional blood cells in the mammalian embryo. Cell reports. 2015; 11:1892–1904. [PubMed: 26095363]

10. de Bruijn MF, Speck NA, Peeters MC, Dzierzak E. Definitive hematopoietic stem cells first develop within the major arterial regions of the mouse embryo. EMBO J. 2000; 19:2465–2474. [PubMed: 10835345]

11. Keller G. Embryonic stem cell differentiation: emergence of a new era in biology and medicine. Genes & development. 2005; 19:1129–1155. [PubMed: 15905405]

12. Murry CE, Keller G. Differentiation of embryonic stem cells to clinically relevant populations: lessons from embryonic development. Cell. 2008; 132:661–680. [PubMed: 18295582]

13. Porcher C, Chagraoui H, Kristiansen MS. SCL/TAL1: a multifaceted regulator from blood development to disease. Blood. 2017; 129:2051–2060. [PubMed: 28179281]

14. Lancrin C, et al. The haemangioblast generates haematopoietic cells through a haemogenic endothelium stage. Nature. 2009; 457:892–895. [PubMed: 19182774]

15. Pijuan-Sala B, et al. A single-cell molecular map of mouse gastrulation and early organogenesis. Nature. 2019; 566:490–495. [PubMed: 30787436]

16. Porcher C, et al. The T cell leukemia oncoprotein SCL/tal-1 is essential for development of all hematopoietic lineages. Cell. 1996; 86:47–57. [PubMed: 8689686]

17. Shivdasani RA, Mayer EL, Orkin SH. Absence of blood formation in mice lacking the T-cell leukaemia oncoprotein tal-1/SCL. Nature. 1995; 373:432–434. [PubMed: 7830794]

18. de Bruijn M, Dzierzak E. Runx transcription factors in the development and function of the definitive hematopoietic system. Blood. 2017; 129:2061–2069. [PubMed: 28179276]

19. Huber TL, Kouskoff V, Fehling HJ, Palis J, Keller G. Haemangioblast commitment is initiated in the primitive streak of the mouse embryo. Nature. 2004; 432:625–630. [PubMed: 15577911]

20. Lugus JJ, Park C, Ma YD, Choi K. Both primitive and definitive blood cells are derived from Flk-1+ mesoderm. Blood. 2009; 113:563–566. [PubMed: 18957687]

21. Arnold SJ, Sugnaseelan J, Groszer M, Srinivas S, Robertson EJ. Generation and analysis of a mouse line harboring GFP in the Eomes/Tbr2 locus. Genesis. 2009; 47:775–781. [PubMed: 19830823]

22. Soriano P. Generalized lacZ expression with the ROSA26 Cre reporter strain. Nature genetics. 1999; 21:70. [PubMed: 9916792]

23. Arnold SJ, Hofmann UK, Bikoff EK, Robertson EJ. Pivotal roles for eomesodermin during axis formation, epithelium-to-mesenchyme transition and endoderm specification in the mouse. Development. 2008; 135:501–511. [PubMed: 18171685]

24. Shalaby F, et al. Failure of blood-island formation and vasculogenesis in Flk-1-deficient mice. Nature. 1995; 376:62–66. [PubMed: 7596435]

25. Lee D, et al. ER71 acts downstream of BMP, Notch, and Wnt signaling in blood and vessel progenitor specification. Cell Stem Cell. 2008; 2:497–507. [PubMed: 18462699]

26. Koyano-Nakagawa N, Garry DJ. Etv2 as an essential regulator of mesodermal lineage development. Cardiovasc Res. 2017; 113:1294–1306. [PubMed: 28859300]

27. Nostro MC, Cheng X, Keller GM, Gadue P. Wnt, activin, and BMP signaling regulate distinct stages in the developmental pathway from embryonic stem cells to blood. Cell stem cell. 2008; 2:60–71. [PubMed: 18371422]

28. Irion S, et al. Temporal specification of blood progenitors from mouse embryonic stem cells and induced pluripotent stem cells. Development. 2010; 137:2829–2839. [PubMed: 20659975]

29. Chagraoui H, et al. SCL/TAL1 cooperates with Polycomb RYBP-PRC1 to suppress alternative lineages in blood-fated cells. Nat Commun. 2018; 9:5375. [PubMed: 30560907]

30. Mikkola HK, Fujiwara Y, Schlaeger TM, Traver D, Orkin SH. Expression of CD41 marks the initiation of definitive hematopoiesis in the mouse embryo. Blood. 2003; 101:508–516. [PubMed: 12393529]

31. Kattman SJ, et al. Stage-specific optimization of activin/nodal and BMP signaling promotes cardiac differentiation of mouse and human pluripotent stem cell lines. Cell stem cell. 2011; 8:228–240. [PubMed: 21295278]

32. Izumi N, Era T, Akimaru H, Yasunaga M, Nishikawa S. Dissecting the molecular hierarchy for mesendoderm differentiation through a combination of embryonic stem cell culture and RNA interference. Stem Cells. 2007; 25:1664–1674. [PubMed: 17446562]

33. Mitjavila-Garcia MT, et al. Expression of CD41 on hematopoietic progenitors derived from embryonic hematopoietic cells. Development. 2002; 129:2003–2013. [PubMed: 11934866]

34. Ferkowicz MJ, et al. CD41 expression defines the onset of primitive and definitive hematopoiesis in the murine embryo. Development. 2003; 130:4393–4403. [PubMed: 12900455]

35. Costello I, et al. The T-box transcription factor Eomesodermin acts upstream of Mesp1 to specify cardiac mesoderm during mouse gastrulation. Nature cell biology. 2011; 13:1084–1091. [PubMed: 21822279]

36. Van Den Ameele J, et al. Eomesodermin induces Mesp1 expression and cardiac differentiation from embryonic stem cells in the absence of Activin. EMBO reports. 2012; 13:355–362. [PubMed: 22402664]

37. Clarke RL, et al. The expression of Sox17 identifies and regulates hemogenic endothelium. Nature cell biology. 2013; 15:502. [PubMed: 23604320]

38. Buenrostro JD, Giresi PG, Zaba LC, Chang HY, Greenleaf WJ. Transposition of native chromatin for fast and sensitive epigenomic profiling of open chromatin, DNA-binding proteins and nucleosome position. Nat Methods. 2013; 10:1213–1218. [PubMed: 24097267]

39. Org T, et al. Scl binds to primed enhancers in mesoderm to regulate hematopoietic and cardiac fate divergence. EMBO J. 2015; 34:759–777. [PubMed: 25564442]

40. Schutte J, et al. An experimentally validated network of nine haematopoietic transcription factors reveals mechanisms of cell state stability. Elife. 2016; 5

41. Onodera K, et al. GATA-1 transcription is controlled by distinct regulatory mechanisms during primitive and definitive erythropoiesis. Proc Natl Acad Sci U S A. 1997; 94:4487–4492. [PubMed: 9114016]

42. Teo AKK, et al. Pluripotency factors regulate definitive endoderm specification through eomesodermin. Genes & development. 2011; 25:238–250. [PubMed: 21245162]

43. Vijayaragavan K, et al. Noncanonical Wnt signaling orchestrates early developmental events toward hematopoietic cell fate from human embryonic stem cells. Cell Stem Cell. 2009; 4:248–262. [PubMed: 19265664]

44. Ng ES, et al. The primitive streak gene Mixl1 is required for efficient haematopoiesis and BMP4-induced ventral mesoderm patterning in differentiating ES cells. Development. 2005; 132:873–884. [PubMed: 15673572]

45. DiMartino JF, et al. The Hox cofactor and proto-oncogene Pbx1 is required for maintenance of definitive hematopoiesis in the fetal liver. Blood. 2001; 98:618–626. [PubMed: 11468159]

46. Fleury M, Eliades A, Carlsson P, Lacaud G, Kouskoff V. FOXF1 inhibits hematopoietic lineage commitment during early mesoderm specification. Development. 2015; 142:3307–3320. [PubMed: 26293303]

47. Wang M, et al. MEIS2 regulates endothelial to hematopoietic transition of human embryonic stem cells by targeting TAL1. Stem Cell Res Ther. 2018; 9:340. [PubMed: 30526668]

48. Davenport TG, Jerome-Majewska LA, Papaioannou VE. Mammary gland, limb and yolk sac defects in mice lacking Tbx3, the gene mutated in human ulnar mammary syndrome. Development. 2003; 130:2263–2273. [PubMed: 12668638]

49. Goode DK, et al. Dynamic Gene Regulatory Networks Drive Hematopoietic Specification and Differentiation. Dev Cell. 2016; 36:572–587. [PubMed: 26923725]

50. Wang Q, et al. The p53 Family Coordinates Wnt and Nodal Inputs in Mesendodermal Differentiation of Embryonic Stem Cells. Cell Stem Cell. 2017; 20:70–86. [PubMed: 27889317]

51. Tosic J, et al. Eomes and Brachyury control pluripotency exit and germ-layer segregation by changing the chromatin state. Nat Cell Biol. 2019; 21:1518–1531. [PubMed: 31792383]

52. Lie ALM, et al. Regulation of RUNX1 dosage is crucial for efficient blood formation from hemogenic endothelium. Development. 2018; 145

53. Fitch SR, et al. Gata3 targets Runx1 in the embryonic haematopoietic stem cell niche. IUBMB Life. 2020; 72:45–52. [PubMed: 31634421]

54. Butler A, Hoffman P, Smibert P, Papalexi E, Satija R. Integrating single-cell transcriptomic data across different conditions, technologies, and species. Nat Biotechnol. 2018; 36:411–420. [PubMed: 29608179]

55. Eliades A, et al. The Hemogenic Competence of Endothelial Progenitors Is Restricted by Runx1 Silencing during Embryonic Development. Cell Rep. 2016; 15:2185–2199. [PubMed: 27239041]

56. Tober J, Yzaguirre AD, Piwarzyk E, Speck NA. Distinct temporal requirements for Runx1 in hematopoietic progenitors and stem cells. Development. 2013; 140:3765–3776. [PubMed: 23924635]

57. Yzaguirre AD, Howell ED, Li Y, Liu Z, Speck NA. Runx1 is sufficient for blood cell formation from non-hemogenic endothelial cells in vivo only during early embryogenesis. Development. 2018; 145

58. Swiers G, et al. Early dynamic fate changes in haemogenic endothelium characterized at the single-cell level. Nat Commun. 2013; 4

59. Obier N, et al. Cooperative binding of AP-1 and TEAD4 modulates the balance between vascular smooth muscle and hemogenic cell fate. Development. 2016; 143:4324–4340. [PubMed: 27802171]

60. Padron-Barthe L, et al. Clonal analysis identifies hemogenic endothelium as the source of the blood-endothelial common lineage in the mouse embryo. Blood. 2014; 124:2523–2532. [PubMed: 25139355]

61. Behringer, R, Gertsenstein, M, Nagy, KV, Nagy, A. Manipulating the Mouse Embryo: A Laboratory Manual. Cold Spring Harbor Laboratory Press; 2014.

62. DiTacchio L, et al. Transcription factors ER71/ETV2 and SOX9 participate in a positive feedback loop in fetal and adult mouse testis. J Biol Chem. 2012; 287:23657–23666. [PubMed: 22613723]

63. Wang Q, et al. Disruption of the Cbfa2 gene causes necrosis and hemorrhaging in the central nervous system and blocks definitive hematopoiesis. Proc Natl Acad Sci U S A. 1996; 93:3444–3449. [PubMed: 8622955]

64. Dobin A, et al. STAR: ultrafast universal RNA-seq aligner. Bioinformatics. 2013; 29:15–21. [PubMed: 23104886]

65. Love MI, Huber W, Anders S. Moderated estimation of fold change and dispersion for RNA-seq data with DESeq2. Genome biology. 2014; 15:550. [PubMed: 25516281]

66. Stuart T, et al. Comprehensive Integration of Single-Cell Data. Cell. 2019; 177:1888–1902 e1821. [PubMed: 31178118]

67. McCarthy DJ, Campbell KR, Lun AT, Wills QF. Scater: pre-processing, quality control, normalization and visualization of single-cell RNA-seq data in R. Bioinformatics. 2017; 33:1179–1186. [PubMed: 28088763]

68. Lun AT, McCarthy DJ, Marioni JC. A step-by-step workflow for low-level analysis of single-cell RNA-seq data with Bioconductor. F1000Res. 2016; 5

69. Langmead B, Salzberg SL. Fast gapped-read alignment with Bowtie 2. Nat Methods. 2012; 9:357–359. [PubMed: 22388286]

70. Li H, et al. The Sequence Alignment/Map format and SAMtools. Bioinformatics. 2009; 25:2078–2079. [PubMed: 19505943]

71. Ramirez F, et al. deepTools2: a next generation web server for deep-sequencing data analysis. Nucleic Acids Res. 2016; 44:W160–165. [PubMed: 27079975]

72. Zhang Y, et al. Model-based analysis of ChIP-Seq (MACS). Genome Biol. 2008; 9:R137. [PubMed: 18798982]

73. McLean CY, et al. GREAT improves functional interpretation of cis-regulatory regions. Nat Biotechnol. 2010; 28:495–501. [PubMed: 20436461]

74. McLeay RC, Bailey TL. Motif Enrichment Analysis: a unified framework and an evaluation on ChIP data. BMC Bioinformatics. 2010; 11:165. [PubMed: 20356413]

75. Zhao H, et al. CrossMap: a versatile tool for coordinate conversion between genome assemblies. Bioinformatics. 2014; 30:1006–1007. [PubMed: 24351709]

76. Quinlan AR, Hall IM. BEDTools: a flexible suite of utilities for comparing genomic features. Bioinformatics. 2010; 26:841–842. [PubMed: 20110278]

77. Robinson JT, et al. Integrative genomics viewer. Nat Biotechnol. 2011; 29:24–26. [PubMed: 21221095]

78. Stemmer M, Thumberger T, Del Sol Keyer M, Wittbrodt J, Mateo JL. CCTop: An Intuitive, Flexible and Reliable CRISPR/Cas9 Target Prediction Tool. PLoS One. 2015; 10

79. Hsu PD, et al. DNA targeting specificity of RNA-guided Cas9 nucleases. Nat Biotechnol. 2013; 31:827–832. [PubMed: 23873081]

80. Heinz S, et al. Simple combinations of lineage-determining transcription factors prime cis-regulatory elements required for macrophage and B cell identities. Mol Cell. 2010; 38:576–589. [PubMed: 20513432]

81. Senft AD, et al. Combinatorial Smad2/3 Activities Downstream of Nodal Signaling Maintain Embryonic/Extra-Embryonic Cell Identities during Lineage Priming. Cell Rep. 2018; 24:1977–1985. [PubMed: 30134160]
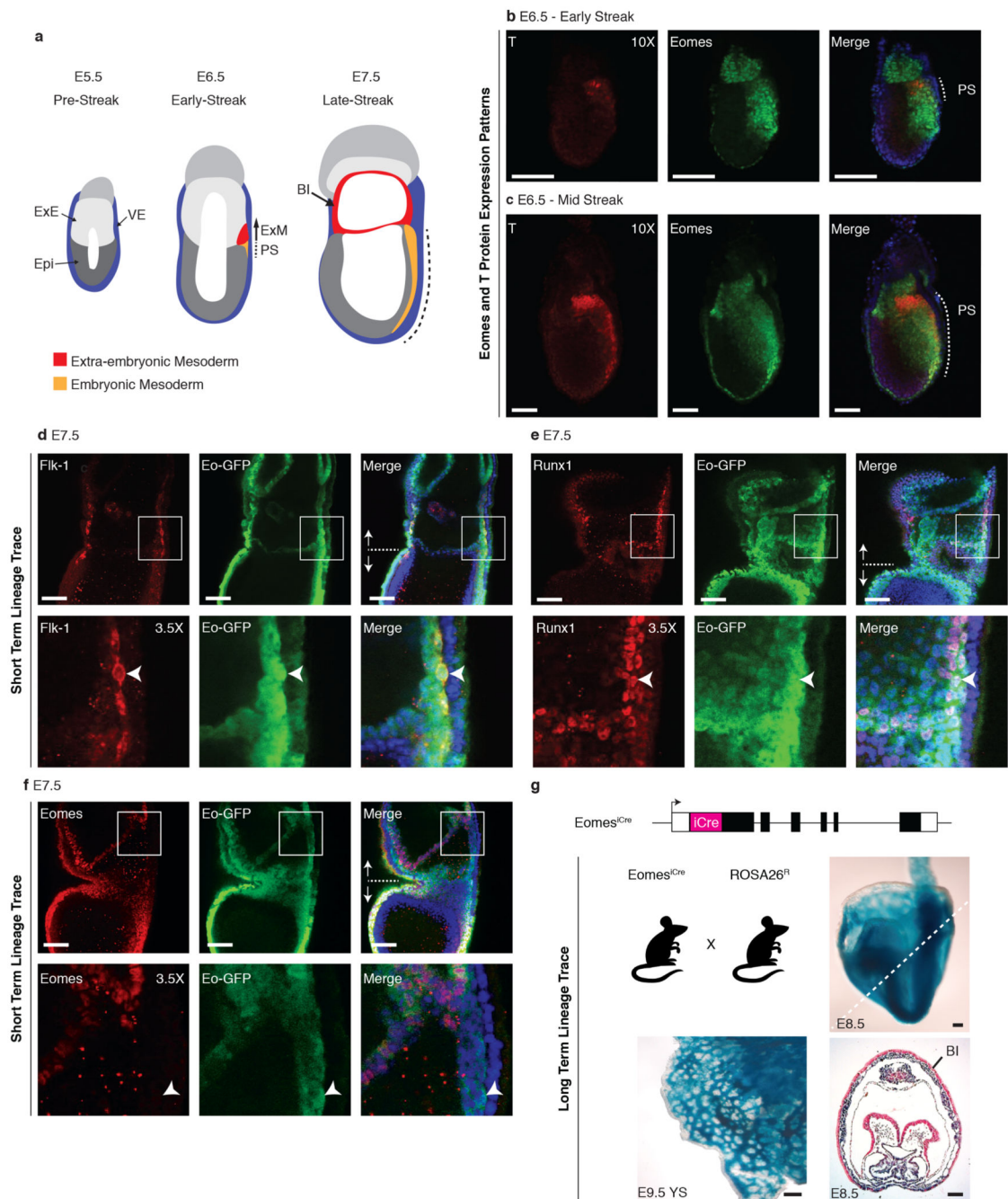
Figure 1. Eomes is expressed in extraembryonic mesodermal progenitors that give rise to yolk-sac hematopoietic and vascular cells.

a, Schematic representation of mouse gastrulation. Extra-embryonic mesoderm (ExM) progenitors migrate proximally from the primitive streak (PS, dotted line) and give rise to the blood islands (BI) of the developing yolk-sac (YS). ExE, extraembryonic ectoderm; Epi, epiblast; VE, visceral endoderm. **b, c,** Early/mid streak stage embryos (E6.5) stained for Brachyury (red) and Eomes (green) and counterstained with DAPI (blue); Images representative of 19 embryos (E6.5) and 19 embryos (E7.5). The length of the PS is denoted

by the dotted line. **d - f,** Immunofluorescence staining of E7.5 Eomes [GFP/+21] embryos for Flk-1(**d**, red; 11 embryos), Runx1(**e**, red; 11 embryos), Eomes (**f**, red 6 embryos) and Eomes-GFP (**d-f**, green). Nuclei are stained with DAPI (blue). Dotted white lines indicate the extraembryonic/embryonic boundary. White boxes denote the zoomed in areas displayed in the lower panels. **g,** Descendants of Eomes[iCre] expressing cells give rise to hematopoietic and endothelial cells of the YS BI. Mice carrying an improved Cre recombinase (iCre) inserted into the ATG start site at the Eomes locus were crossed to ROSA26[R] reporter mice that express LacZ upon Cre induced recombination. Wholemount X-gal staining was performed on E8.5 and E9.5 embryos and sections were counterstained with nuclear fast-red to highlight non-labelled cells; Images representative of at least 3 embryos. Scale bars, 100 μM.
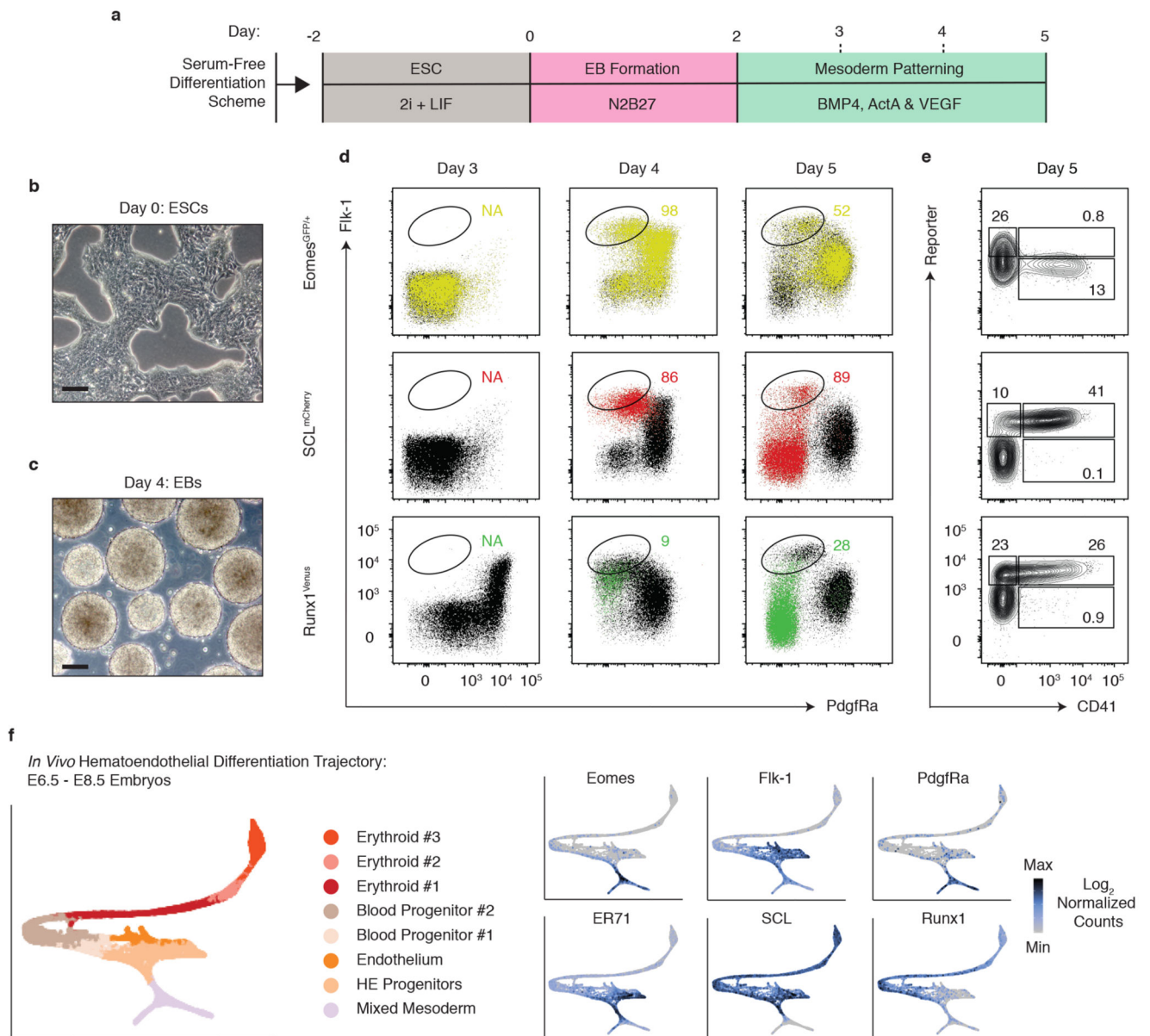
Figure 2. Eomes, SCL and Runx1 expression during hematopoietic development *in vitro* and *in vivo*.
a, Schematic representation of the ESC differentiation protocol. **b, c,** Representative phase contrast photomicrographs at day 0 **(b)** and day 4 **(c)** of the differentiation protocol; Images representative of at least 3 independent differentiations. Scale bars, 100 μM. Embryoid body, EB. **d,** Flow cytometric analysis of EB cultures generated from Eomes, SCL and Runx1 reporter ESC lines. Cells expressing the indicated fluorescent reporters are shown by coloured dots. Eomes-GFP, yellow; SCL-mCherry, red; Runx1-Venus, green. The percentages of reporter positive cells within the circled Flk-1^{hi}/PdgfRa$^-$ cell population are indicated (1 differentiation performed). **e,** Analysis of day 5 EBs showing fluorescent reporter activity and expression of the hematopoietic marker CD41 (1 differentiation performed). **f,** Force-directed graph layout of cells isolated from E6.5 to E8.5 embryos

associated with the blood/endothelial lineage (adapted from Pijuan-Sala et al. 2019)[15]. Left plot highlights various cell-types that are generated along the hematovascular lineage trajectory as mesoderm differentiates into endothelial and hematopoietic cells. Right plots are overlaid with Log_2 normalized gene expression levels. HE, hematoendothelial.
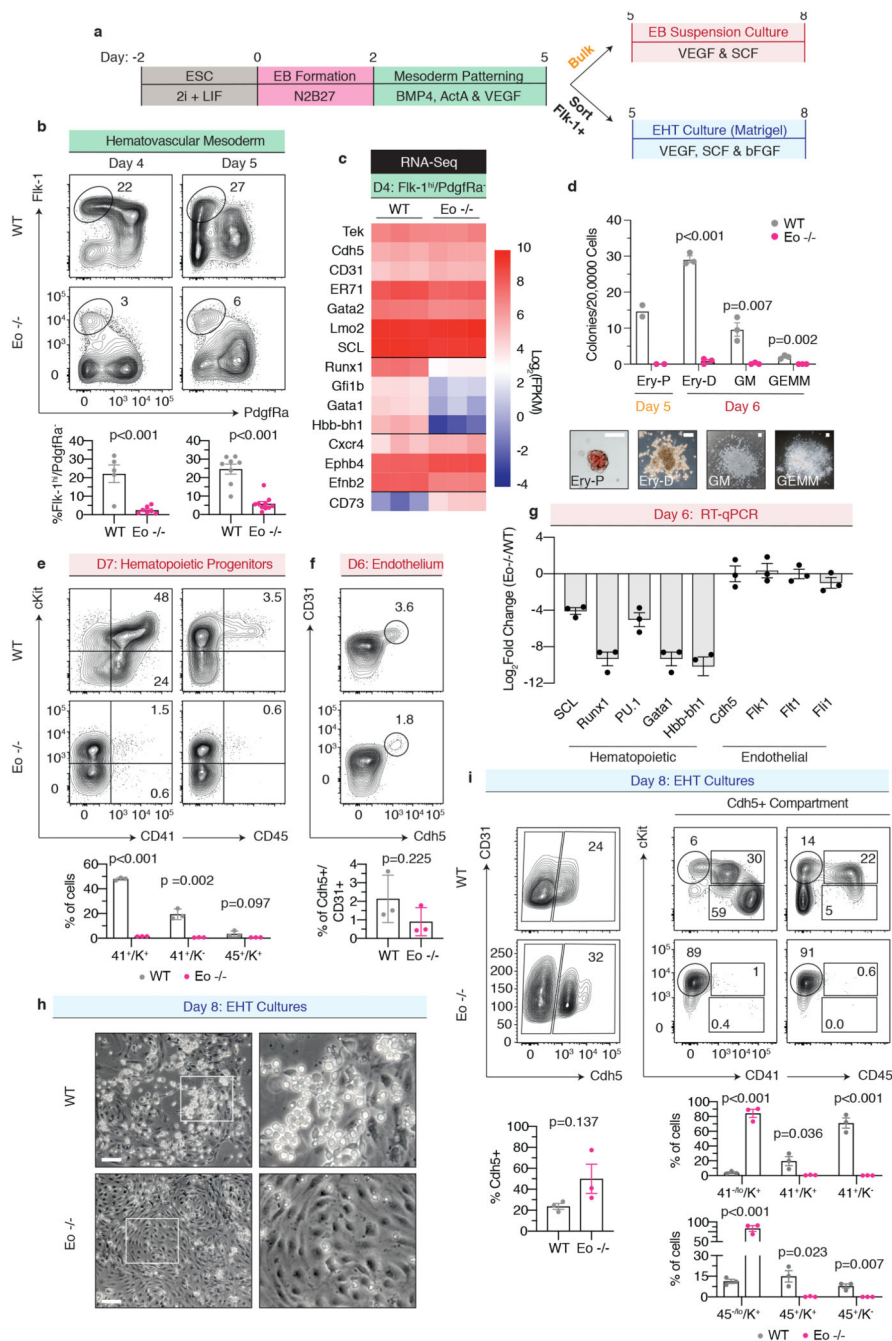
Figure 3. Eomes functional loss disrupts primitive and definitive hematopoiesis but not endothelial development

a, ESC differentiation protocols modelling yolk-sac hematopoiesis differ from day 5 onwards (EB suspension culture, red and EHT culture, blue). **b,** Representative flow cytometric analysis of Flk-1/PdgfRa expression in wild-type (WT) and Eomes^{-/-} EBs at day 4/5. Graphical data indicate the mean +/- SEM; n = 5 (WT D4), n = 7 (Eomes^{-/-} D4), n = 8 (WT D5) amd n = 10 (Eomes^{-/-} D5) independent differentiations. **c,** Heatmap showing Log2(FPKM) expression of hematovascular genes in day 4 WT and Eomes^{-/-} Flk-1^{hi}/

PdgfRa⁻ cells from n = 3 independent differentiations. **d**, Hematopoietic potential of cells isolated from day5/6 WT and Eomes⁻/⁻ EBs plated in hematopoietic colony-forming assays. Graphical data indicate mean +/- SEM; n = 2 (day 5) and n = 3 (day 6) biologically independent samples. Ery-P, primitive erythrocyte; Ery-D, definitive erythrocyte; GM, granulocyte-macrophage; GEMM, granulocyte-erythro-myeloid. Scale bar, 100 μM. **e**, Representative flow cytometric analysis of cKit/CD41 and cKit/CD45 expression in day 7 WT and Eomes⁻/⁻ EBs. Graphical data indicate mean +/- SEM; n = 3 biologically independent samples. **f,** Representative flow cytometric analysis of Cdh5/CD31 expression in day 6 WT and Eomes⁻/⁻ EBs. Graphical data indicate mean +/- SEM; n = 3 biologically independent samples. **g,** Log$_2$Fold Change (Eomes⁻/⁻ versus WT) of hematovascular marker gene expression in day 6 EB cultures determined using reverse transcription quantitative PCR (RT-qPCR); mean +/- SEM; n = 3 biologically independent samples. GAPDH was used as a housekeeping gene. **h,** Representative phase contrast images of day 8 WT and Eomes⁻/⁻ EHT cultures; Representative of 3 independent differentiations. Scale bars, 100 μM **i,** Representative flow cytometric analysis of Cdh5 expression and cKit/CD41 or cKit/CD45 expression within the Cdh5+ compartment in day 8 WT and Eomes⁻/⁻ EHT cultures. Graphical data indicate mean +/- SEM; n = 3 independent differentiations. For all graphical representations of flow cytometry/colony-forming data individual replicates are shown as coloured dots (WT = grey, Eomes⁻/⁻ = pink). Statistical analyses were performed using two-tailed unpaired Student's t-tests. Statistical source data are provided in Source Data Fig. 3.
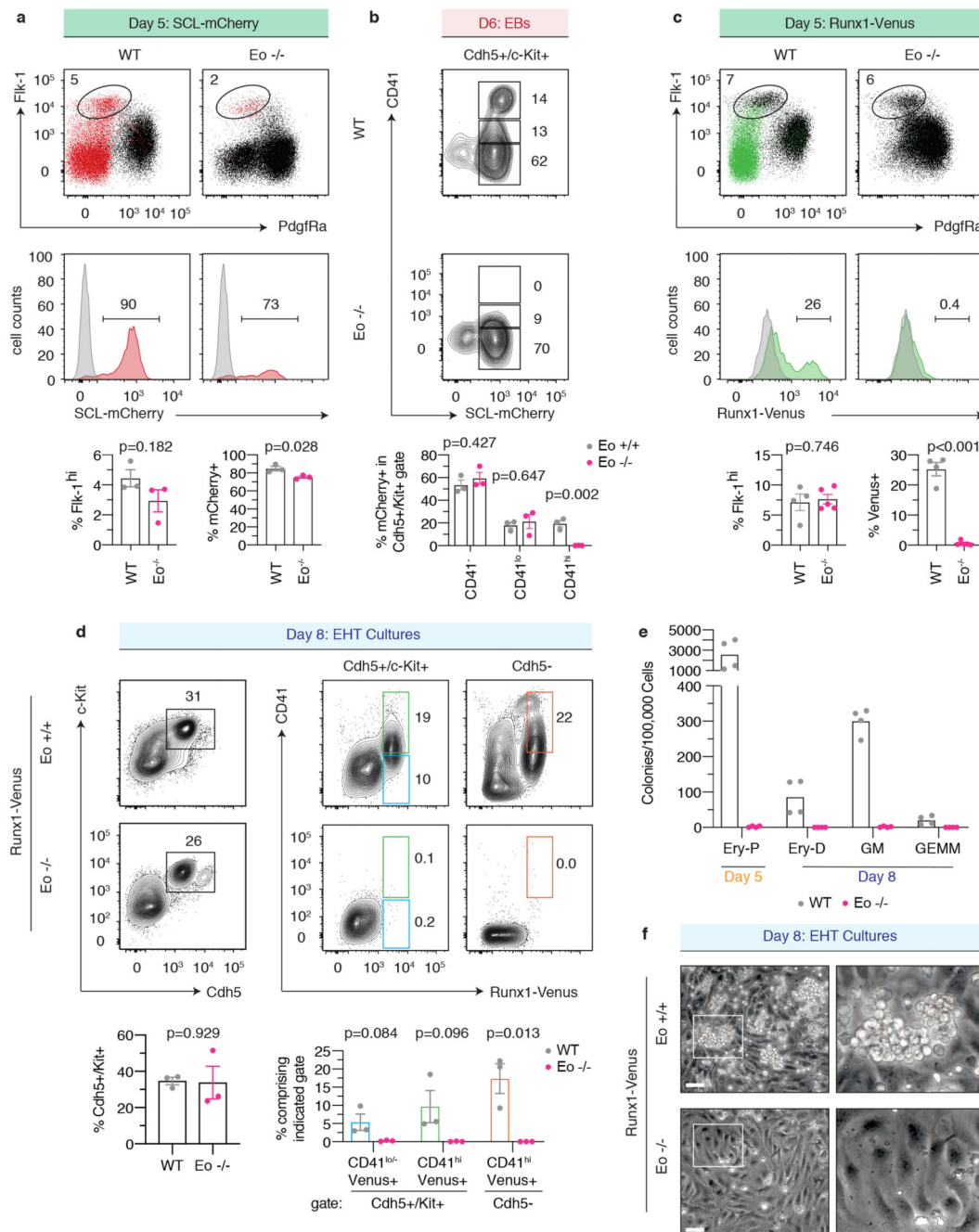
Figure 4. Eomes-null cultures lack Runx1+ hemogenic endothelial cells

a,c, Representative flow cytometric analysis of Flk-1/PdgfRa and SCL-mCherry (**a**) or Runx1-Venus (**c**) expression in day 5 WT and Eomes$^{-/-}$ EBs. Coloured dots indicate cells positive for the expression of fluorescent reporters. SCL-mCherry, red; Runx1-Venus, green. Histograms display SCL-mCherry (**a**) and Runx1-Venus (**c**) expression levels in the Flk-1^{hi}/PdgfRa$^-$ compartment; grey peaks depict expression in a control cell line. Graphical data indicate mean +/- SEM; n = 3 (WT and Eomes$^{-/-}$ SCL-mCherry), n = 4 (WT Runx1-Venus) and n = 5 (Eomes$^{-/-}$ Runx1-Venus) independent differentiations. **b**, Representative flow

cytometric analysis of CD41/SCL-mCherry expression within the Cdh5$^+$/c-Kit$^+$ compartment in day 6 WT SCL-mCherry and Eomes-/- SCL-mCherry EBs. Graphical representations display mean +/- SEM; n = 3 independent differentiations. **d,** Representative flow cytometric analysis of Cdh5/cKit expression (left) and Runx1-Venus/CD41 expression within the Cdh5$^+$/cKit$^+$ (middle) and Cdh5$^-$ (right) compartments in day 8 WT and Eomes$^{-/-}$ EHT cultures. Graphical representations indicate mean +/- SEM; n = 3 independent differentiations. **e**, Hematopoietic colony-forming potential of cells isolated from day 5 bulk EBs and day 8 EHT cultures plated in hematopoietic colony assays. Each dot displays the number of colonies formed in each technical replicate from n=2 independent differentiations; 2 technical replicates/independent differentiation. Ery-P, primitive erythrocyte; Ery-D, definitive erythrocyte; GM, granulocyte-macrophage; GEMM, granulocyte-erythro-myeloid. **f,** Representative phase contrast images of Runx1-Venus Eomes$^{+/+}$ and Runx1-Venus Eomes$^{-/-}$ EHT cultures at day 8; 3 independent differentiations. Scale bars, 100 μM. For all graphical representations of flow cytometry individual replicates are shown as coloured dots (Eomes$^{+/+}$ = grey and Eomes$^{-/-}$ = pink). Statistical analyses were performed using unpaired two-tailed Student's t-tests. Statistical source data are provided in Source Data Fig. 4.
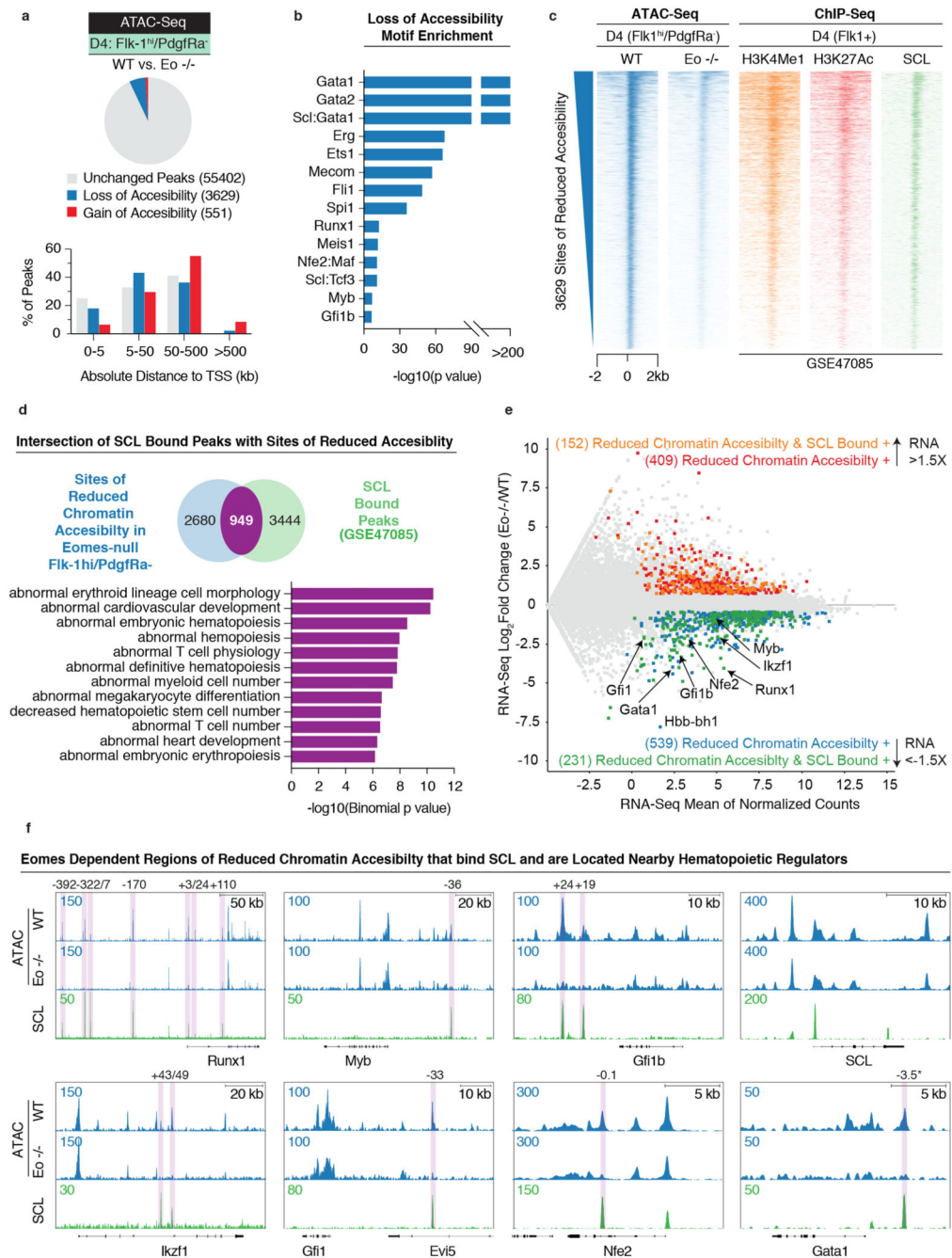
Figure 5. Eomes regulates chromatin accessibility at SCL bound cis-regulatory regions
a, Pie chart depicting the proportion of ATAC peaks that lose (blue) or gain (red) chromatin accessibility in Eomes$^{-/-}$ day 4 Flk-1^{hi}/PdgfRa$^-$ cells. Bar chart depicting the distribution of ATAC peaks located nearby transcriptional start sites (TSS) with unchanged (grey), reduced (blue) or increased (red) chromatin accessibility in day 4 Eomes$^{-/-}$ vs. WT Flk-1^{hi}/PdgfRa$^-$ cells; n = 3 independent differentiations. **b,** Sites of reduced chromatin accessibility in Eomes$^{-/-}$ cells are enriched for hematopoietic TF binding motifs. Statistical analyses were performed using *AME* (Analysis of Motif Enrichment). **c,** Heatmaps showing ATAC signals

from WT (blue, left) or Eomes$^{-/-}$ (blue, right) day 4 Flk-1^{hi}/PdgfRa$^-$ cells and ChIP signal for H3K4Me1 (orange), H3K27Ac (red) and SCL (green) occupancy from day 4 WT Flk-1$^+$ cells[39]. Heatmaps show a 4kb flanking region surrounding sites of reduced chromatin accessibility in day 4 Eomes$^{-/-}$ Flk-1^{hi}/PdgfRa$^-$cells. **d,** Venn diagram depicting the overlap of SCL bound regions[39] and sites of reduced chromatin accessibility. Enriched GO Terms in the Mouse Phenotype category for the 949 shared genomic regions (purple). Statistical analyses were performed using *GREAT* (Genomic Regions Enrichment Analysis Tool). **e,** MA plot highlighting genes that are differentially expressed in Eomes$^{-/-}$ and WT hematovascular mesoderm (Flk-1^{hi}/PdgfRa$^-$) that have nearby sites of reduced chromatin accessibility (red and blue squares) that are also bound by SCL in WT Flk-1$^+$ mesoderm[39] (orange and green squares). **f,** IGV snapshots of ATAC-Seq (blue) and ChIP-Seq (green) tracks highlighting hematopoietic regulators that have nearby genomic regions with reduced chromatin accessibility in Eomes$^{-/-}$ Flk-1^{hi}/PdgfRa$^-$cells that are also bound by SCL[39] in WT Flk-1$^+$ mesoderm are highlighted by purple bars. Numbers above the purple bars indicate the relative location of these sites in kilobases to the TSS of the indicated genes. (*the -3.5 enhancer at the Gata1 locus was called as a peak by MACS2 (p<0.05) in only the WT Flk-1^{hi}/PdgfRa$^-$ samples)
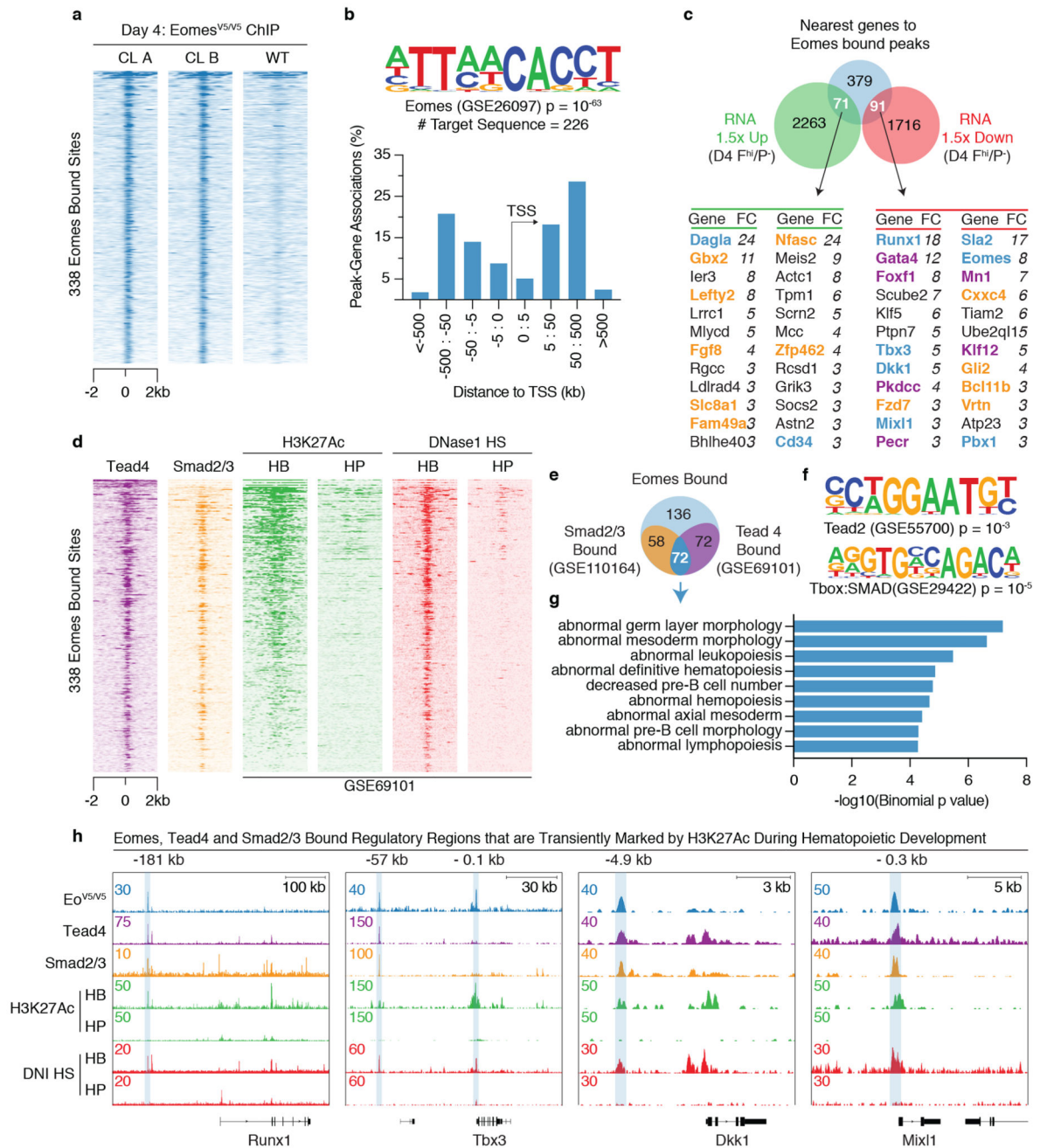
Figure 6. Genomic regions transiently marked by H3K27Ac are bound by Eomes, Tead4 and Smad2/3 during early stages of hematopoietic mesoderm development.
a, Heatmaps of ChIP peaks in a 4kb region from day 4 EBs from two independent Eomes[V5/V5] clones. **b,** An Eomes consensus binding motif[42] identified using HOMER is enriched under ChIP-Seq peaks (top). Bar graph (below) depicts the distribution of ChIP-Seq peaks relative to nearby transcriptional start sites. **c,** Venn diagram showing the overlap between ChIP-Seq peak associated genes and those differentially expressed (fold change >1.5X) in the Eomes^{-/-} Flk-1^{hi}/PdgfRa[-] hematovascular mesoderm population. The top 24

genes having associated ChIP-Seq peaks significantly upregulated (green, left) or downregulated (red, right) in Eomes$^{-/-}$ versus WT day 4 Flk-1^{hi}/PdgfRa$^-$ hematovascular mesoderm are listed. Numbers indicate the fold change (FC). Orange genes have nearby Smad2/3/Eomes overlapping peaks, purple genes have nearby Tead4/Eomes overlapping peaks and blue genes have nearby Tead4/Eomes/Smad2/3 overlapping peaks. **d**, Heatmaps showing ChIP-Seq signal for Tead4 (purple)[49] and Smad2/3 (orange)[50] occupancy in day 3 or day 4 Flk-1$^+$ EB cultures, respectively. Heatmaps showing ChIP-Seq signal for H3K27Ac (green) histone modifications in hemangioblast (HB) and hematopoietic (HP) cells[49]. Heatmaps showing DNAseI hypersensitivity signal in hemangioblast (HB) and hematopoietic (HP) cells[49]. All heatmaps show a 4kb region flanking peak centres of the 338 Eomes bound sites. **e,** Venn diagram depicting the overlap of the Eomes, Smad2/3 and Tead4 bound regions. **f,** Tead2 and Tbox:Smad motifs identified using *HOMER* that are significantly enriched under the Eomes bound ChIP-Seq peaks. **g,** Enriched GO Terms in the Mouse Phenotype category for the 72 Eomes, Smad2/3 and Tead4 overlapping genomic regions (blue). Statistical analyses were performed using *GREAT* (Genomic Regions Enrichment Analysis Tool) **h**, IGV snapshots of Eomes, Tead4, Smad2/3 and H3K27Ac ChIP-Seq peaks overlapping with DNase1 hypersensitivity (DN1 HS). Blue bars highlight Eomes bound sites and the numbers above indicate the relative location of these sites in kilobases to the TSS of the gene indicated. HB, hemangioblast (T$^+$/Flk-1$^+$); HP, hematopoietic progenitor (CD41$^+$).
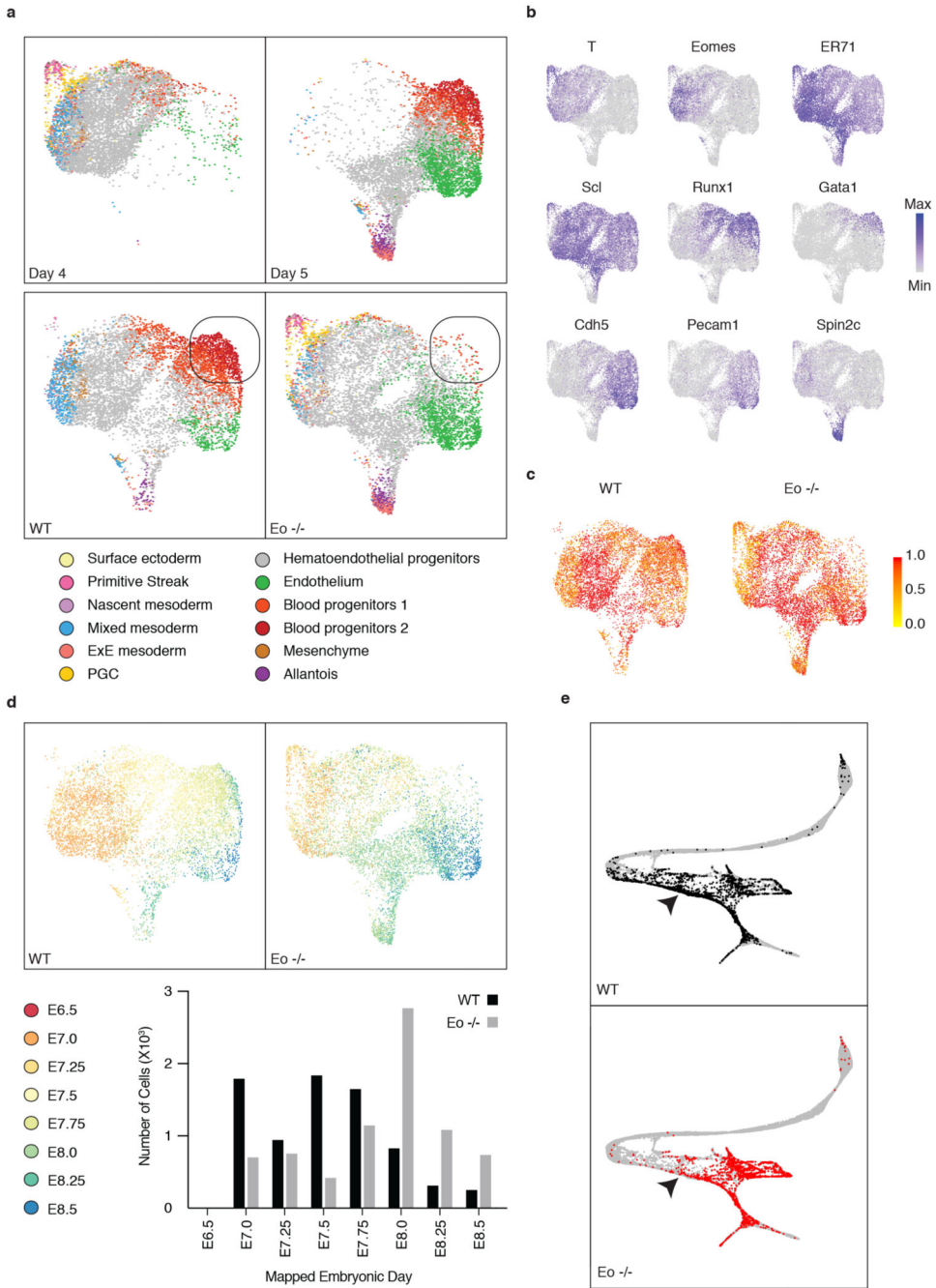
Figure 7. Comparison of scRNA-Seq profiles of wildtype and Eomes-null Flk1^{hi}/PdgfRa$^-$ cells generated *in vitro* to wildtype cells from E6.5 - E8.5 mouse embryos.

a, Mapped cell types in uniform manifold approximation and projection (UMAP) plots. Top panel shows WT and Eo-/- Flk-1^{hi}/PdgfRa$^-$ cells from either day 4 (left) or day 5 (right). Bottom panel shows Flk-1^{hi}/PdgfRa$^-$ cells from WT (left) or Eomes$^{-/-}$ (right). Cells are colored by their cell type annotation, based on their 35 nearest neighbors in the mouse gastrulation atlas[15] denoted in the legend. The black box (bottom panel) highlights blood progenitors that are diminished in the Eomes$^{-/-}$cultures. PGC, primordial germ cell; WT,

wildtype; Eo -/-, Eomes-null **b,** Normalized expression levels of the indicated genes overlaid on UMAPs for all cells. **c,** Mapped probability mapping scores in UMAP embeddings for all wildtype (left) and Eomes-/- (right) cells. A probability score >0.5 indicates high mapping quality. **d,** Mapped embryo stages in UMAP embeddings. Cells are coloured by the nearest mapped embryo stage from the mouse atlas as indicated in the legend below. Bar chart shows the number of wildtype (black) or Eomes-/- (grey) cells from each mapped embryo stage. E, embryonic stage. **e,** Mapping day 4/5 Flk-1^{hi}/PdgfRa[-] wildtype (top) and Eomes-/- (bottom) cells onto the blood-related differentiation trajectory[15]. The black arrowhead denotes the point at which hematopoietic development seems to be blocked in Eomes-/- cultures.
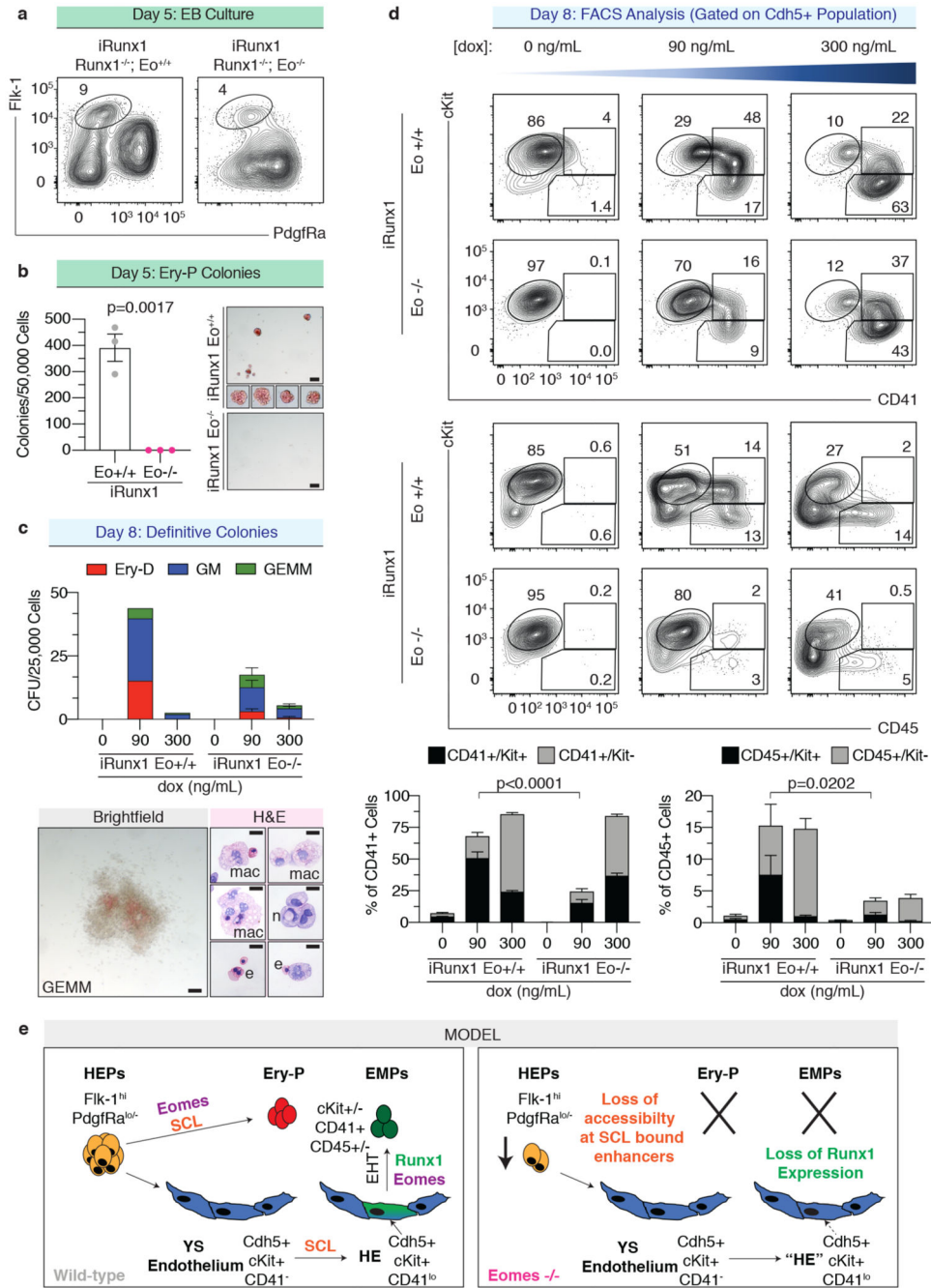
Figure 8. Runx1 re-expression in Eomes-null/Runx1-null EHT cultures rescues definitive hematopoiesis.

a, Flow cytometric analysis of Flk-1/PdgfRa expression in day 5 iRunx1 Eomes^{+/+} and iRunx1 Eomes^{-/-} EBs. **b,** Hematopoietic colony-forming potential of cells isolated from day 5 iRunx1 Eomes [+/+] and iRunx1 Eomes^{-/-} EBs. Graphical representation displays mean +/- SEM; n=3 independent differentiations [and representative photomicrographs are shown on the right. Ery-P, primitive erythrocyte. Scale bar, 100 μM. Statistical analysis was performed using a two-tailed unpaired Student's t-test. **c,** Hematopoietic colony-forming potential of

day 8 EHT cultures in which Runx1 expression was uninduced/induced via addition of 0, 90 and 300 ng/mL of dox from day 6-8. Graphical representations display mean +/- SEM; n = 2 (iRunx1 Eomes+/+) and n = 3 (iRunx1 Eomes -/-) independent differentiations. Ery-D, definitive erythrocyte; GM, granulocyte-macrophage; GEMM, granulocyte-erythrocyte-myeloid. H&E stained hematopoietic cells (bottom right) from a representative GEMM colony (brightfield, bottom left) from a dox induced iRunx1 Eomes$^{-/-}$ EHT culture. Mac, macrophage; n, neutrophil; e, erythrocyte. Scale bars: brightfield,100 μM; H&E, 20μM. **d,** Representative flow cytometric analyses of cKit/CD41 and cKit/CD45 expression within the Cdh5+ compartment of day 8 EHT cultures in which Runx1 expression was uninduced or induced via addition of 0, 90 and 300 ng/mL of dox from day 6-8. Graphical representations indicate mean +/- SEM; Representative of at least 3 independent differentiations. Statistical analyses were performed using a 2-way ANOVA and Tukey's multiple comparison test. Statistical source data are provided in Source Data Fig. 8. **e,** Model summarizing the effects of Eomes-loss-of-function on the two waves of YS hematopoiesis. Primitive erythrocyte formation depends on SCL and Eomes functional activity. The generation of hemogenic endothelium (HE) depends on SCL functional activity. EHT and the generation of definitive hematopoietic cells depends on the functional activity of Runx1 and Eomes. Eomes-/- hematoendothelial progenitors (HEPs) lack chromatin accessibility at numerous enhancers that are normally bound by SCL and are therefore unable to transition into primitive erythrocytes. Eomes$^{-/-}$ hematoendothelial progenitors generate Cdh5+/cKit+/CD41^{lo} "hemogenic" endothelial cells that fail to upregulate Runx1 expression (green) and this in part explains the block in definitive hematopoiesis in Eomes$^{-/-}$ EHT cultures.